Chinese Chemical Letters 37 (2026) 111956

Contents lists available at ScienceDirect

Chinese Chemical Letters

journal homepage: www.elsevier.com/locate/cclet

Artificial intelligence-driven personalized clinical decision-making and drug development in breast cancer

Ting Wang[a], Xifeng Qin[a], Yao Liu[b], Jianhui Tian[b,*], Zhiqing Pang[a,*]

[a] School of Pharmacy, Key Laboratory of Smart Drug Delivery, Ministry of Education, Fudan University, Shanghai 201203, China
[b] Clinical Oncology Center, Shanghai Municipal Hospital of Traditional Chinese Medicine, Shanghai University of Traditional Chinese Medicine, Shanghai 200071, China

ARTICLE INFO

Article history:
Received 5 June 2025
Revised 12 October 2025
Accepted 13 October 2025
Available online 14 October 2025

Keywords:
Artificial intelligence
Breast cancer
Personalized treatment
Clinical decision-making
Drug development

ABSTRACT

Breast cancer (BRCA) is a multifaceted and extremely diverse condition, with conventional diagnostic and therapeutic methods encountering considerable obstacles. With the increasing amount of medical data and the ongoing development of computer technologies, artificial intelligence (AI) has become widely used in BRCA medication research and clinical decision-making. Specifically, AI helps anticipate therapy responses, makes it easier to choose the best treatment regimens based on the molecular and pathological features of tumors, and allows for more accurate risk assessments for BRCA. AI is also essential to drug development, including the identification and prediction of novel therapeutic targets, the screening and prediction of compound structures, the repurposing of existing drugs, and the creation of combination treatments. From static assessments based on molecular subtypes to dynamic tracking of disease development, AI's role in BRCA diagnosis and therapy has changed throughout time. It has transitioned from experience-based therapeutic approaches to data-driven clinical decision-making. In addition to improving patients' quality of life, this shift is essential to turning cancer therapy into a "prevention-prediction-personalized" paradigm. This review article thoroughly examines the developments in AI applications for important fields such as molecular subtype identification, metastasis and recurrence prediction, BRCA risk stratification, and the creation of new medications. It delves deeper into current technological constraints and clinical translation pathways, emphasizing the need for advances in clinical applicability and technical standardization through tactics like large-scale multi-center clinical trials, innovative cross-modal data integration, and algorithmic architecture optimization.

© 2026 Published by Elsevier B.V. on behalf of Chinese Chemical Society and Institute of Materia Medica, Chinese Academy of Medical Sciences.

1. Introduction

Artificial intelligence (AI) is a multidisciplinary domain aimed at empowering computer systems to do activities often necessitating human intelligence [1]. It integrates perspectives from several fields. Machine learning (ML) and deep learning (DL), the two main technologies underlying AI, are sometimes confused with one another, but it's crucial to recognize that DL is a subset of ML [2]. ML employs mathematical algorithms to identify patterns in data, subsequently utilized for making predictions [3]. Prominent approaches in ML encompass conventional methods such as support vector machines (SVMs), decision trees (DT), and K-means clustering. These strategies aim to emulate the human capacity for pattern recognition. Nonetheless, in comparison to DL, they often need a greater duration for training and evaluation on certain tasks. For example, although DT may effectively categorize data, they include a significant limitation: too intricate trees may overfit the data, whereas overly simplified trees do not adequately capture essential patterns. Random forest (RF), a method based on DT, addresses some of these issues by combining multiple trees and incorporating randomness in both data selection and feature selection. Extreme gradient boosting (XGBoost) is an innovative approach that creates an ensemble of DT and offers several advantages compared to conventional logistic regression (LR) models. This encompasses enhanced management of absent data, the capacity to model non-linear associations among variables, and superior effectiveness in addressing intricate interactions between characteristics [4]. DL utilizes multi-layered neural networks, modeled after the brain's architecture, to generate predictions. For instance, convolutional neural networks (CNNs), a fundamental technique in DL, have gained extensive utilization in medical image analysis based on their remarkable feature extraction capabilities and ro-

* Corresponding authors.
E-mail addresses: tjhhawk@shutcm.edu.cn (J. Tian), zqpang@fudan.edu.cn (Z. Pang).

https://doi.org/10.1016/j.cclet.2025.111956
1001-8417/© 2026 Published by Elsevier B.V. on behalf of Chinese Chemical Society and Institute of Materia Medica, Chinese Academy of Medical Sciences.

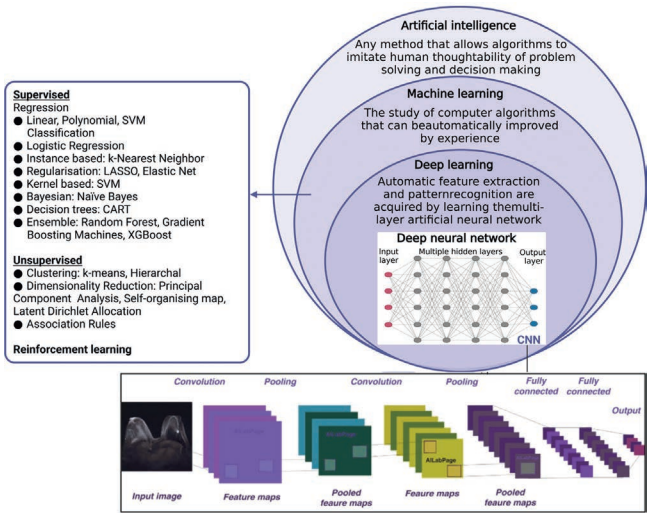


Fig. 1. The domains of AI technology, the interconnections among AI, ML, and DL, together with instances of frequently utilized algorithms. Reproduced with permission [5]. Copyright 2023, Springer Nature.

bust adaptability to spatial data (Fig. 1) [5]. DL has demonstrated significant efficacy in managing extensive and intricate datasets, including pictures, audio, and text. It autonomously acquires characteristics from unprocessed data, diminishing the necessity for laborious feature engineering. Still, a significant issue associated with DL models is their deficiency in interpretability, rendering it arduous to comprehend the rationale behind the model's results [6].

Breast cancer (BRCA) is among the most common malignancies worldwide [7], accounting for 31 % of all cancer incidences in women [8,9]. Over the past two decades, the death rate for women due to BRCA has steadily increased. As per the 2022 global cancer statistics, BRCA holds the highest rates of incidence (24.5 %) and death (15.5 %) among women [10,11]. The treatment of BRCA often entails a comprehensive strategy. With the rapid advancement of biological data gathering and computational technologies, AI methodologies are progressively employed to provide comprehensive analytical frameworks for clinical BRCA data.

In BRCA research, these AI technologies are tailored to clinical needs: SVMs leverage their high-dimensional classification strengths to predict human epidermal growth factor receptor 2 (HER2) status, a critical small-sample nonlinear task. RF, valued for feature significance output, supports feature selection and survival analysis (*e.g.*, random survival forest (RSF) models for metastatic risk prediction). XGBoost and light gradient boosting machine (LightGBM) facilitate multi-modal data fusion (*e.g.*, recurrence risk prediction) *via* their strengths in missing value handling and parallel processing. For straightforward probability predictions like preoperative HER2-low status evaluation, LR, a linear classifier, offers strong interpretability. DL models extend these capabilities: CNN-based ResNet and U-Net enable automated magnetic resonance imaging (MRI) feature extraction and pathology slide segmentation, respectively; recurrent neural networks (RNNs) process time-series data to dynamically track disease progression (*e.g.*, mid-treatment chemotherapy efficacy); Transformers, *via* attention mechanisms, excel in long-sequence and cross-modal tasks such as drug-target interaction (DTI) prediction and pathological image interpretation. Generative adversarial networks (GANs) address rare subtype sample scarcity by generating synthetic data (*e.g.*, triple-negative breast cancer (TNBC) pathology images), while graph neural networks (GNNs) model molecular and gene-drug networks to predict drug synergies. TabNet integrates attention and sparse feature selection for end-to-end tabular data processing (*e.g.*, preoperative lymph node metastasis prediction), and stacking ensemble models (*e.g.*, SVM + RF) enhance accuracy in multi-modal fusion tasks like chemotherapy response prediction.

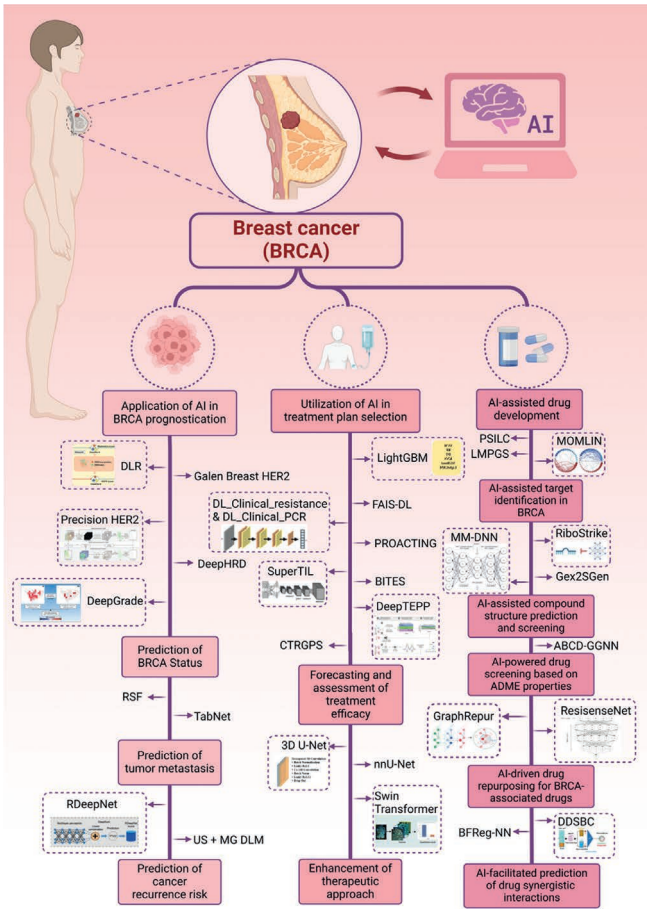


Fig. 2. Framework for AI applications in BRCA. Created with BioRender.com. The names of important AI models from each part of the main text are shown in the figure along with the schematic designs that go with them.

The capacity of AI to revolutionize clinical decision-making and the drug development process is becoming evident. Simultaneous advancements will enable breakthroughs in BRCA tumor prediction, therapy selection, and pharmaceutical research and development. Here we will review recent advancements in the domains of AI-driven personalized clinical decision-making and drug development in BRCA (Fig. 2).

2. Application of AI in BRCA prognostication

AI has significantly improved the diagnosis and treatment of BRCA by forecasting tumor status, metastasis, and recurrence risks. The primary clinical advantage is in enabling early intervention, customized treatment, and efficient resource allocation through accurate prediction and stratification, hence enhancing patients' quality of life and extending lifespan. Table S1 (Supporting information) presents a summary of the AI models employed for BRCA prognostication prediction. BRCA is categorized using several factors, including molecular traits like estrogen receptor/progesterone receptor (ER/PR), HER2, and Ki-67; clinical aspects like age, hormone status, and tumor node metastasis (TNM) staging; and histological classifications including ductal carcinoma *in situ* (DCIS) and invasive ductal carcinoma (IDC) [12]. Across these several domains, AI has shown remarkable ability in predicting tumor sta-

tus. This study will concentrate on the identification of HER2-low, HER2 scoring, risk assessment of DCIS, homologous recombination deficiency (HRD) testing, and histological grading, aiming to furnish substantial support for precision medicine [13–19]. Models such as RSF, TabNet, and the SVM model integrating breast-specific gamma imaging (BSGI) and ultrasound, along with those specifically designed for NAT (neoadjuvant therapy) patients [20–25], have demonstrated improved prediction accuracy, diminished reliance on invasive procedures, and enhanced patient management in the context of tumor metastasis prediction. In the domain of forecasting tumor recurrence risk, models like RDeepNet [26], those integrating multimodal imaging with clinical data [27], and the XGBoost model utilize MRI data [28], multimodal imaging, and clinical characteristics to deliver precise predictions. These models facilitate individualized treatment strategies and enhance prognostic outcomes, ultimately advancing precision medicine in BRCA.

2.1. Prediction of BRCA status

Molecular subtypes of BRCA exhibit significant variety, resulting in distinct therapeutic approaches and prognostic outcomes. HER2-low BRCA accounts for approximately 45 % to 55 % of all primary BRCAs and is categorized as HER2-negative based on current HER2 testing protocols. This classification indicates that HER2-targeted therapies are generally not advised or are ineffective for these patients [29,30]. Regardless, the innovative antibody-drug combination, trastuzumab deruxtecan, has shown promise in the treatment of HER2-low metastatic BRCA [31]. Consequently, choosing the best course of therapy and forecasting the prognosis of patients depend on correctly distinguishing HER2-low BRCA from HER2-negative BRCA. Currently, HER2 expression status is often evaluated using immunohistochemistry (IHC) or *in situ* hybridization (ISH) methods [32–34]. However, these methods do come with some significant drawbacks. The variability in HER2 expression frequently results in the misdiagnosis of HER2-low BRCA as either HER2-negative or HER2-positive in invasive core needle biopsies. Moreover, these techniques are intrusive and may produce incorrect outcomes if the tissue specimen is inadequate or of substandard quality. Furthermore, HER2 status may vary throughout the therapy process or as the illness advances. Thus, the development of a non-invasive technique that can rapidly and precisely determine HER2 status is urgently needed. Chen *et al*. performed groundbreaking work investigating the efficacy of ML models for preoperative prediction of HER2-low BRCA [19], utilizing radiomic characteristics obtained from contrast-enhanced cone-beam breast computed tomography (CE-CBBCT). This advanced imaging technique has several benefits compared to conventional approaches, including high spatial resolution three-dimensional (3D) imaging, rapid data collection, and the capability to thoroughly depict lesion morphology, calcifications, and enhancement patterns [35]. A total of 1046 quantitative radiomic characteristics were collected from CE-CBBCT images and standardized utilizing z-scores in the study. Key characteristics were identified by Pearson correlation coefficients and recursive feature removal. Six ML models were created based on the chosen features: linear discriminant analysis (LDA), RF, SVM, LR, AdaBoost (AB), and DT. The models were chiefly assessed utilizing receiver operating characteristic (ROC) curves and the area under the curve (AUC). Alongside AUC, many additional measures such as accuracy, Matthews correlation coefficient, specificity, sensitivity, positive predictive value (PPV), and negative predictive value (NPV) were employed to thoroughly evaluate the models' performance. Among the evaluated models, LDA and LR had the highest AUC values (0.880) in the validation cohort, signifying robust efficacy in differentiating HER2-low from HER2-negative BRCA. The LDA model had a superior AUC and attained a better accuracy of 0.872, in contrast to the LR model's 0.846, indicating a marginal performance advantage. In contrast, the DT model showed a lower AUC (0.713), which could be the result of overfitting. The results indicate that LDA and LR are the most efficacious models for predicting HER2-low BRCA, presumably owing to their capacity to handle linear correlations and yield interpretable outcomes. The study revealed that ML models utilizing CE-CBBCT radiomic characteristics have superior efficacy in preoperatively predicting HER2-low BRCA. These models offer a non-invasive method to evaluate HER2 status, potentially facilitating more precise and individualized targeted therapies. Also, their prognostic skills may aid doctors in optimizing treatment decisions and facilitate patient recruitment for anti-HER2 clinical trials, particularly when re-evaluating HER2 expression in resistant advanced subtypes. Although these results are encouraging, more confirmation with larger sample numbers is necessary; yet, they indicate a potential trajectory for the future of precision therapy in HER2-low BRCA.

Deep semantic segmentation feature-based radiomics (DSFR), is a deep semantic segmentation-based feature that Guo *et al*. combined with conventional MRI radiomic characteristics to create and verify the deep learning radiomics (DLR) model [18]. This model non-invasively detects HER2-low positive status in BRCA patients and forecasts disease-free survival (DFS) by averaging the probability generated by two distinct models. In comparison to the radiomics model (AUC = 0.705) and the DSFR model (AUC = 0.867), the DLR model exhibited enhanced diagnostic performance in the training cohort (AUC = 0.868) and yielded comparable findings in the validation cohort. The DLR model outperformed both the classic radiomics model and the DSFR model in differentiating between HER2-low positive and HER2-negative patients, hence improving the precision of HER2 status evaluation. Finally, the DLR model demonstrated reliable prediction accuracy across diverse lesion types and hormone receptor statuses, indicating robust generalization capacities. Survival study indicated that the HER2-low positive status predicted by the DLR model correlated with extended DFS, hence reinforcing the therapeutic significance of its predictions.

HER2 expression levels are categorized into four classifications: HER2 3+, 2+, 1+, and 0 [29]. Attaining a more accurate assessment of HER2 expression necessitates the assistance of systematic AI models. Two researchers have utilized AI to improve the precision and uniformity of HER2 IHC scoring. To assist pathologists in evaluating HER2 IHC scores in BRCA, Krishnamurthy *et al*. presented a completely automated AI method [17]. This multicenter, two-arm, multi-reader research encompassed 120 HER2 IHC whole-slide pictures. Four pathologists evaluated the pictures both with and without AI aid, and these evaluations were compared to a high-confidence benchmark truth, created by a minimum of four breast pathology subspecialists in accordance with the American Society of Clinical Oncology/College of American Pathologists (ASCO/CAP) 2018/2023 standards. The AI model, Galen Breast HER2, created by ibex medical analytics, autonomously executes functions including the detection of tissue fragments, identification of invasive tumor locations, classification of tumor cells, and computation of HER2 scores in accordance with ASCO/CAP recommendations (Fig. 3A). The utilization of the AI tool resulted in enhanced performance by readers. Interobserver agreement increased from 75.0 % with the digital manual reading to 83.7 % with AI-assisted review, while scoring accuracy improved from 85.3 % to 88.0 %. Precision HER2, a complete, high-precision AI system, was created by Xiong *et al*. to accurately and consistently assess HER2 expression in invasive breast cancer (IBC) [14]. This investigation encompassed a two-phase validation process: in the initial phase, pathologists analyzed HER2 whole-slide pictures unaided by AI; two weeks later, they re-evaluated the identical slides utilizing the AI system. The AI model autonomously detected and eliminated DCIS components by Calponin staining and utilized image overlay techniques to remove

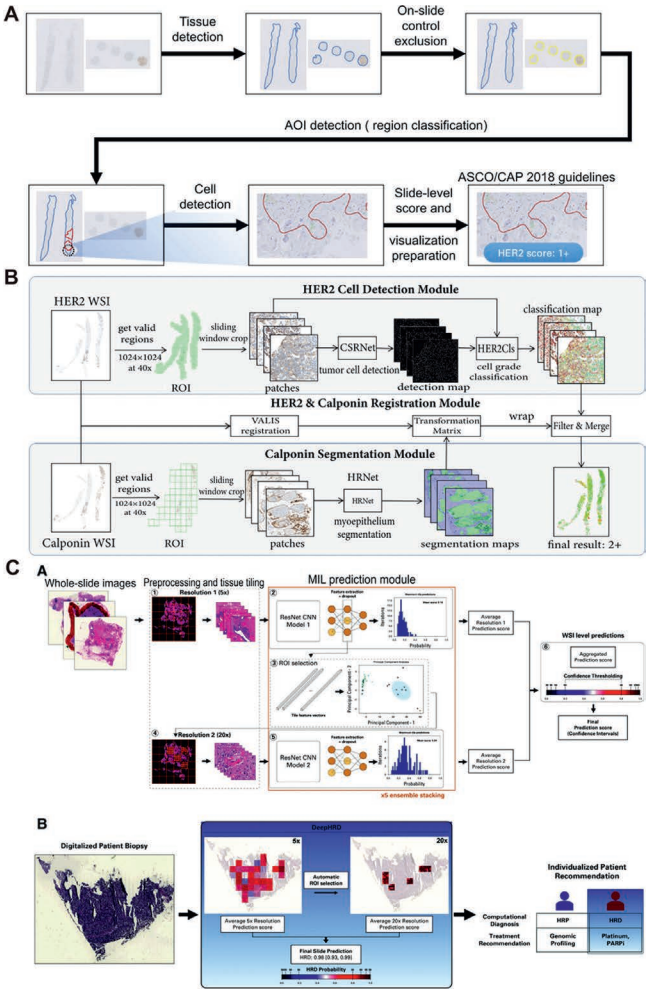


Fig. 3. Representative AI models for BRCA status prediction. (A) Overview of a fully automated AI algorithm for HER2 immunohistochemical scoring in BRCA. Reproduced with permission [17]. Copyright 2024, Wolters Kluwer Health. (B) Framework of the AI detection for HER2 and myoepithelium. Reproduced with permission [14]. Copyright 2024, Springer Nature. (C) A multiresolution CNN architecture to detect HRD from histopathologic tissue slides. Reproduced with permission [13]. Copyright 2024, Wolters Kluwer Health.

these components from the HER2-stained slides. This method enhanced the precision of HER2 scoring in invasive carcinoma tissue (Fig. 3B). The technology markedly improved reading accuracy (0.902 *vs.* 0.710) and decreased the misclassification of HER2 1+ as HER2 0 (32/279 *vs.* 65/279), enabling patients to receive antibody-drug conjugates (ADCs). It enhanced HER2 score consistency across pathologists of varying experience levels (intra-class correlation coefficient (ICC): 0.872–0.926 *vs.* 0.818–0.908), particularly benefiting those with less expertise (0.885 *vs.* 0.818). This indicates that AI can mitigate discrepancies arising from subjective judgment disparities among pathologists. Both research projects concentrate on employing AI to improve the precision and uniformity of HER2 scoring. The initial research underscores AI as a completely automated instrument that enhances scoring precision and uniformity while also emphasizing its extensive application in diverse laboratory environments. The second research, conversely, emphasizes the unique advantages of AI in enhancing scoring precision and uniformity, especially in managing DCIS components and reducing scoring disparities across various pathologists.

Similar challenges of diagnostic subjectivity arise in the evaluation of pre-invasive lesions. For instance, DCIS risk stratification relies heavily on histopathological interpretation. The prompt diagnosis of BRCA poses a considerable therapeutic challenge, especially in the detection and treatment of DCIS. DCIS is a non-invasive variant of BRCA that, although it seldom advances to invasive cancer in the majority of instances [36], nonetheless presents a risk of progression in some situations [29,36]. Accordingly, precise grading and risk evaluation of DCIS are essential for informing treatment choices. Alaeikhanehshir *et al.* did a study to investigate the use of DL in mammography for differentiating between low-risk and high-risk DCIS [16], offering significant decision-making assistance for patients under active monitoring. The researchers utilized a U-Net-based CNN for this objective. U-Net is a prevalent DL architecture utilized in medical picture segmentation [37]. Metrics, including the area under the ROC curve and predictive values, which offer an objective assessment of the model's capacity to distinguish between high-risk and low-risk DCIS, were used to assess the classification performance. Two principal performance metrics, the PPV and NPV, were employed to assess the model's accuracy in predicting high-risk and low-risk DCIS, respectively. The findings indicated that when categorizing DCIS as high-risk, the DL network attained a PPV of 0.40, an NPV of 0.91, and an AUC of 0.72 on the test dataset. When differentiating high-risk and/or upgraded DCIS from low-risk DCIS, the PPV rose to 0.80, the NPV to 0.84, and the AUC to 0.76. This indicates that the CNN exhibited outstanding accuracy in differentiating between low-grade and high-grade DCIS. The U-Net-based CNN exhibited strong performance, presumably owing to its encoder-decoder architecture, which facilitates the automated learning of high-level image characteristics and their integration with low-level, high-resolution data *via* skip connections, therefore producing high-resolution segmentation masks. This study's CNN not only executed lesion segmentation but also integrated an additional convolutional branch for image-level classification, facilitating concurrent lesion segmentation and risk stratification. This dual function significantly improved the model's predictive performance. Thus, CNNs can function as essential instruments in the therapy of DCIS, augmenting other clinical and pathological information to formulate individualized treatment strategies for patients. Particularly in the context of active monitoring, CNNs can assist doctors in more precisely evaluating DCIS risk, hence enhancing treatment decision-making.

Beyond morphological characterization, AI also enables molecular-level stratification critical for precision therapy. A key example is the prediction of HRD, which dictates targeted treatment selection. In precision oncology [38], the identification of HRD is essential for selecting therapeutic choices in BRCA. Patients with HRD-positive BRCA may exhibit enhanced responsiveness to platinum-based treatments and poly ADP-ribose polymerase (PARP) inhibitors [39]. Conventional HRD detection approaches based on molecular analysis are expensive, time-intensive, and not widely accessible, impeding their wider application in clinical practice and studies [40]. In order to overcome this drawback, Bergstrom *et al.* created DeepHRD [13], a DL platform driven by AI that can directly predict HRD status from standard tissue slides stained with hematoxylin and eosin (H&E). This provides a more effective and economical method of HRD detection. The platform utilizes a poorly supervised CNN design that replicates the diagnostic processes of pathologists. It begins with initial predictions at low magnification and thereafter autonomously identifies areas of interest (ROIs) for enhanced examination at greater magnification (Fig. 3C). The model was trained and validated with data from 1008 BRCA cases and 459 ovarian cancer cases sourced from The Cancer Genome Atlas (TCGA) project. The researchers evaluated the effectiveness of several models by employing ROC curves to compute the AUC, utilizing non-parametric resampling to ascertain confidence intervals, and applying Cox regression analysis to derive hazard ratios. The DeepHRD model attained an AUC of 0.81 in the TCGA BRCA dataset, a finding that was validated in two separate

BRCA cohorts, yielding an AUC of 0.76. In a cohort of metastatic BRCA patients undergoing treatment with platinum-based agents, DeepHRD-predicted HRD cases exhibited markedly elevated complete response rates, accompanied by a 3.7-fold enhancement in median progression-free survival (PFS). DeepHRD found 1.8–3.1 times more HRD patients than conventional molecular detection approaches, who had platinum-specific PFS advantages in metastatic BRCA. These data underscore that DeepHRD represents both a technological advancement and significant therapeutic merit. It offers a cost-effective and swift HRD detection instrument, particularly advantageous in resource-constrained contexts, and delivers essential assistance for clinical decision-making in well-resourced healthcare settings, encompassing treatment planning, alternative therapeutic strategies, and patient recruitment and stratification in clinical trials.

The nottingham histologic hrade (NHG) is a recognized prognostic indicator in BRCA pathology [41,42]. Its grading is constrained, nevertheless, by the considerable variation among assessors, particularly when it comes to tumors categorized as intermediate grade NHG2. Its relevance in informing clinical treatment decisions, especially for NHG2 malignancies, is thus restricted [43–46]. Using DL algorithms based on digital whole-slide pictures, Boissin *et al*. created a unique preoperative breast biopsy risk classification methodology to solve this difficulty [15]. Their objective was to improve the precision of tumor grading and offer more dependable assistance for early treatment decisions. The researchers employed a deep CNN model named DeepGrade, which has been previously validated for risk assessment in excised tumor specimens. This work involved training the DeepGrade model to differentiate between low-risk (NHG1) and high-risk (NHG3) cancers [47], with its performance evaluated against clinical NHG grades. The assessment encompassed metrics like AUC, Cohen's kappa coefficient (which quantifies consistency), sensitivity, and specificity. AUC values nearing 1 signify superior discriminating capability, whilst the kappa coefficient denotes the concordance between the model's predictions and the actual pathology grades. The findings demonstrated that DeepGrade attained a notable AUC of 0.908 in forecasting NHG1 and NHG3 grades in excised tumors, signifying robust prediction accuracy. The algorithm could also further categorize tumors that doctors have categorized as NHG2 into two groups: low-risk (DeepGrade-low) and high-risk (DeepGrade-high). Within NHG2 tumors, 65 % were categorized as DeepGrade-low and 35 % as DeepGrade-high. This is especially important for ER-positive/HER2-negative patients, since those with high-risk malignancies (NHG3) typically get both chemotherapy and endocrine therapy, but those with low-risk tumors (NHG1) may forgo superfluous therapies. The DeepGrade model demonstrated exceptional performance, with its predictions strongly aligning with pathologists' assignments of NHG grades to excised tumor samples, resulting in a kappa value of 0.65, signifying considerable agreement. On the contrary, conventional pathologist grading of biopsy specimens exhibited just 32 % consistency. The DeepGrade model also showed independent prognostic value. Upon controlling for age using a multivariate Cox regression model, the recurrence-free survival (RFS) rate for the DeepGrade-high cohort was markedly inferior to that of the DeepGrade-low cohort. This discovery indicates that DeepGrade enhances tumor grading precision and facilitates early decision-making in clinical practice, potentially mitigating both overtreatment and undertreatment.

2.2. Prediction of tumor metastasis

Metastasis of BRCA continues to be a primary contributor to its elevated death rate [48]. Despite advancements in early identification and therapy, metastatic BRCA remains incurable due to its resistance to almost all existing medications, with the majority of treatments being palliative rather than curative [49]. Conventional predictive approaches, including histological grading and lymph node status, exhibit restricted accuracy in forecasting metastasis and do not completely align with clinical manifestations [50–52]. The implementation of AI may mitigate these constraints. A RSF model was created by Li and associates in order to improve the precision of forecasting the likelihood of BRCA metastases [25]. RSF is an ML methodology that integrates RF with survival analysis. It is not limited by data distribution and is particularly effective for evaluating datasets in which the number of samples is significantly fewer than the number of variables [53]. The authors utilized recursive feature elimination (RF-RFE) to determine the most pertinent predictive factors in their investigation. This technique identifies the elements that most substantially influence prediction accuracy by computing variable importance (VIMP) scores. A variety of assessment indicators were employed to assess the model's prediction efficacy. The assessment encompassed the area under the receiver operating characteristic curve (AUROC) and Kaplan-Meier survival analysis for prediction accuracy, the C-index for evaluating the model's discriminating capacity, and the Brier score for measuring its calibration ability. Collectively, these measures constitute a thorough evaluation framework for assessing model performance. The findings indicated that the prediction model, derived from three principal variables discovered using RSF and RF-RFE (pathological stage, aspartate aminotransferase levels, and neutrophil count), exhibited significant reliability and stability in both the training and validation datasets. The AUROC values were 0.932 and 0.905, the Kaplan-Meier survival analysis indicated $P < 0.0001$, the C-index was 0.959, and the Brier score was 0.097, affirming the model's robust prediction capability. The RSF model showed remarkable efficacy in predicting BRCA metastasis by utilizing standard clinical data and examination measures, owing to its capacity to manage high-dimensional data while preventing overfitting [54–56].

The sentinel lymph node (SLN) biopsy is the conventional surgical method for identifying lymph node metastasis. The SLN is the initial lymph node to which cancer cells disseminate from the original tumor [57], and its status is vital for evaluating the prognosis of BRCA patients and informing treatment strategies. Traditional SLN biopsy, on the other hand, is an intrusive operation that greatly depends on the expertise and experience of the surgeon and involves the risk of consequences, including lymphedema [58–60]. Meanwhile, SLN biopsy still has a certain false-negative rate (FNR), even for patients who had systemic therapy before surgery [61–63]. It follows that precise prediction of SLN metastases would allow physicians to formulate more individualized treatment strategies, reduce superfluous invasive interventions, and improve the patient's treatment experience and overall prognosis. In this regard, Shahriarirad *et al*. created a non-invasive prediction model using the TabNet architecture [24]. Using an attention transformer module in conjunction with sparse feature selection techniques, this end-to-end DL system analyzed multidimensional preoperative data of patients with BRCA, including demographic data, pregnancy-related parameters, laboratory results, and tumor characteristics [64]. In key performance parameters, the model showed notable gains over conventional LR models: accuracy (75 % *vs.* 70 %), sensitivity (87 % *vs.* 79 %), specificity (70 % *vs.* 65 %), and AUC (0.74 *vs*. 0.70). The most significant predictive factors were vascular invasion (key weight), tumor size, biopsy pathology, age, and family history, according to the model's interpretability mechanism. The heatmap produced by sparse attention illustrated the nonlinear relationships among these features. In contrast to the LR model, which mainly concentrated on linear variables like the age at first pregnancy and PR hormone receptor status, TabNet was more adept at detecting intricate relationships like family history and significant pathological outcomes.

Interestingly, the model's statistical improvement in AUC and 8 % absolute increase in sensitivity indicate that it may provide more trustworthy support for clinical decision-making, especially in lowering the possibility of false negatives for patients who need delayed examinations or have biopsy contraindications. The efficacy of AI-driven forecasts relies on several interrelated elements. A DL system [20], utilizing the ResNet50 architecture pre-trained on ImageNet, was employed to evaluate H&E-stained tissue pictures from BRCA patients to predict SLN status in the intergroup sentinel node meta-analysis (INSEMA) study, which predominantly focused on tubular subtypes of primary BRCA. Despite the model's superior performance on the Mannheim external validation set, it did not demonstrate significantly improved outcomes compared to random chance on the retained test set from INSEMA. Also, its performance on external datasets from TCGA and Regensburg was equivalent to random chance. Clinical classifiers, such as Ki-67 and tumor size, had strong efficacy in the Mannheim cohort but exhibited diminished performance in the INSEMA test set (0.6056) and the Regensburg cohort (0.6238). Integrating outputs from the image analysis model into LR did not enhance performance on the INSEMA test set. These results highlight several influencing factors, including dataset limitations, model generalization ability, the relevance of image features to lymph node status, technical aspects, model selection, integration of clinical parameters, study design blinding, statistical methods, and performance metrics. This highlights the intricate complexities and factors involved in implementing DL methods in healthcare decision-making.

Axillary lymph node dissection (ALND) is a conventional operation in the treatment of BRCA. This procedure may result in consequences including lymphedema, strange feelings, and limited arm motion [65–68]. Thus, avoiding unneeded axillary procedures for individuals who are unlikely to benefit from them and lowering surgical consequences can be achieved with a precise evaluation of the axillary lymph node (ALN) burden before surgery. Ultrasound, mammography, and MRI are the three principal imaging modalities for identifying BRCA. They depend on the physical distinctions between malignant and benign breast tissue [69]. Mammography is the gold standard for cancer screening; nevertheless, it has limits in evaluating ALN status, especially in women with thick breast tissue, where its sensitivity is significantly diminished [70]. MRI has superior sensitivity and specificity for BRCA detection; nevertheless, certain individuals may be unable to undergo the procedure due to factors such as implanted devices, body size, renal insufficiency, or claustrophobia. Ultrasound is beneficial because of its convenience, absence of radiation, cost-effectiveness, and non-invasive nature [71]. Nonetheless, its clinical efficacy is constrained by an elevated false positive rate attributable to discrepancies among operators. Alternative screening techniques are therefore required. BSGI is an innovative molecular imaging modality capable of identifying BRCA at sub-centimeter dimensions and across diverse tissue densities, with a sensitivity reported between 90 % and 96 % [72,73]. BSGI entails the administration of a radioactive tracer (*e.g.*, technetium-99 m selenoprotein) and the utilization of a specialized camera to obtain pictures of the breast [74]. This approach distinguishes tumor cells from normal cells based on their biological activity for the diagnosis of BRCA. BSGI demonstrates high specificity in the diagnosis of ALN metastases [75]. Given this context, research by Cai *et al.* used ML techniques to create a model that could predict ALN metastasis by combining ultrasound characteristics and BSGI traits [23]. The goal was to give more precise treatment choices in clinical practice. The research utilized six distinct ML algorithms: Generalized linear model (GLM), RF, SVM, neural network (NNET), gradient boosting machine (GBM), and XGBoost, employing recursive feature elimination (RFE) to identify the most predictive variables. The findings indicated that the SVM model exhibited superior predictive performance in the test set, achieving an AUC of 0.794, sensitivity of 0.641, specificity of 0.8, PPV of 0.676, NPV of 0.774, and accuracy of 0.737. The measurements validated the superiority of the SVM model in predicting ALN metastasis, particularly in differentiating between metastatic and non-metastatic patients with high precision. This may be ascribed to the SVM's capacity to manage high-dimensional data and non-linear associations. By determining the ideal hyperplane, SVM provides superior generalization in feature space. This model has considerable clinical potential, offering non-invasive predictions with accuracy akin to conventional surgery, which has critical implications for enhancing individualized and minimally IBC treatment.

NAT denotes a supplementary treatment administered prior to primary interventions such as surgery or radiation. For patients with clinically positive ALNs (cN+), NAT has emerged as a pivotal therapeutic strategy [76–78]. The primary aim of NAT is to reduce tumor size and decrease staging before surgery, allowing patients who were previously ineligible for the treatment to qualifyand thereby enhancing the probability of surgical success [79,80]. NAT also enables physicians to evaluate tumor responses to therapy. A pathological full lymph node response (ypN0) is characterized by the complete absence of residual tumors in the ALNs after NAT, serving as a vital metric for assessing treatment efficacy and informing subsequent therapeutic approaches. The ypN0 rate following NAT fluctuates significantly, indicating that several individuals may not necessitate ALND [81–83]. As a consequence, precisely forecasting which individuals are predisposed to getting ypN0 following NAT is crucial for circumventing superfluous ALND and enhancing therapeutic strategies. Using DL and radiomics, Yu *et al.* suggested that dynamic contrast-enhanced magnetic resonance imaging (DCE-MRI) scans performed at various stages of therapy may yield nuanced [22], quantitative data. This method seeks to enhance the precision of predicting the probability of attaining ypN0. The research included ML techniques like LightGBM, SVM, RF, and multilayer perceptron (MLP) to construct risk models (Fig. 4A), which were assessed by 10-fold cross-validation. Among the patients, 61 (38.13 %) attained ypN0 following NAT. The "data fusion" model utilizing SVM had superior performance among the other models, achieving an AUC of 0.986 (95 % combination index (CI): 0.954–1.000), far surpassing the others. This model amalgamates radiomics, DL attributes, and clinical data, with its robust prediction capability presumably deriving from its capacity to synthesize diverse data types, providing a more holistic perspective on the tumor's biological activity and treatment response. This model offers a precise and dynamic approach for evaluating ALN in BRCA care, facilitating individualized treatment regimens. In another work, Zhu *et al.* created a multi-factor AI model to assist in evaluating the response of ALN in patients with BRCA following neoadjuvant chemotherapy (NAC) (Fig. 4B) [21]. The study's ML stacking model integrated longitudinal radiomics information with significant clinical and surgical aspects, establishing a holistic, AI-enhanced surgical workflow. The stacking model showed exceptional efficacy in identifying ALN metastases, achieving an AUC of 0.958 in the original cohort, 0.881 in the external validation cohort, and 0.882 in the prospective cohort. In contrast to single-modal models, the stacking model's incorporation of radiomics characteristics from various time periods and locations enabled a more comprehensive depiction of the tumor and lymph nodes' response to NAC. The findings demonstrated that the AI-assisted surgical approach markedly decreased the FNR in clinical practice, reducing it from 14.88 % with SLN biopsy alone to 4.13 % with AI-assisted surgery. The false negative rate fell significantly when more than two SLNs were excised. The findings indicate that AI-assisted surgical techniques can serve as helpful instruments for assessing ALN response post-NAC, hence reducing needless ALND operations and bearing significant therapeutic consequences.

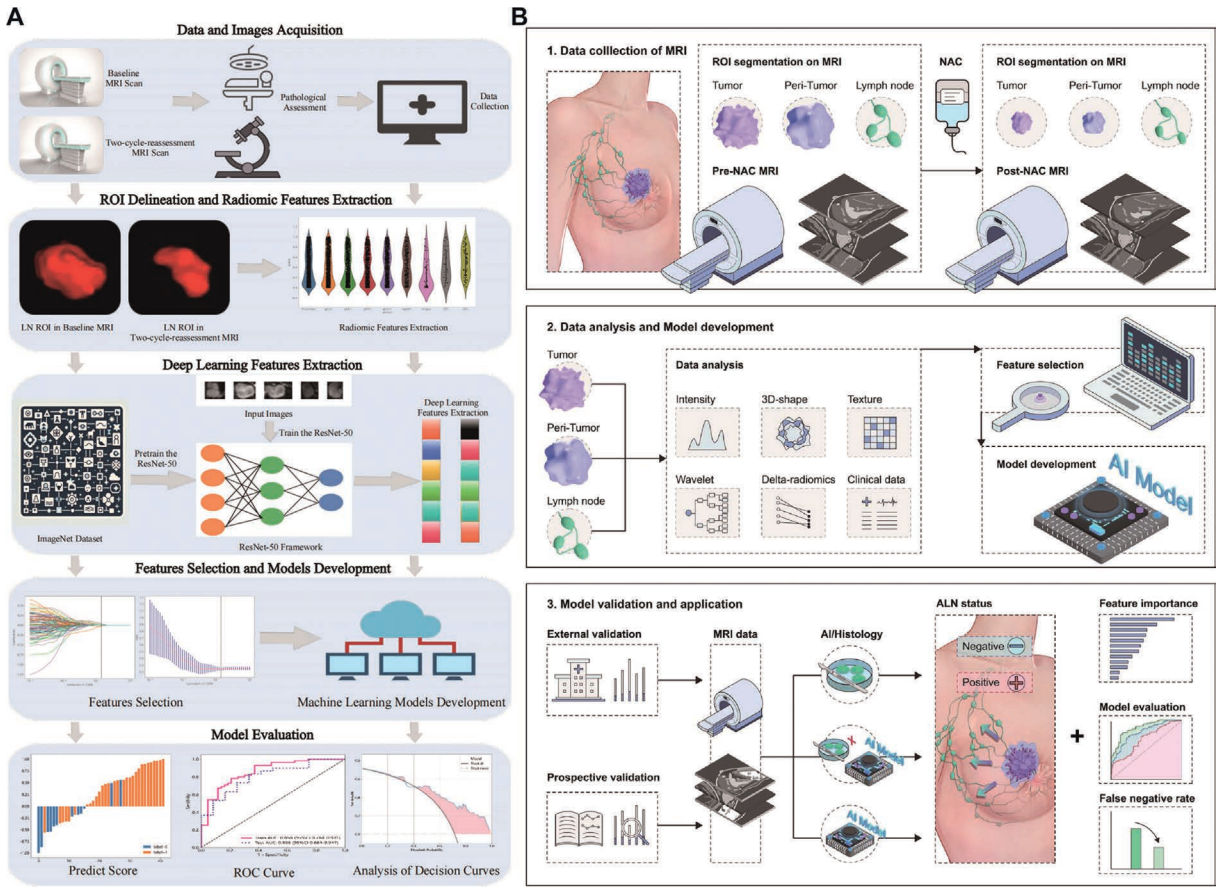


Fig. 4. Representative AI models for BRCA metastasis prediction. (A) Flowchart of ML model development process based on longitudinal DCE-MRI data. Reproduced with permission [22]. Copyright 2024, Elsevier Ltd. (B) Flowchart of ALN surgery assisted by multivariate AI model after NAC for BRCA. Reproduced with permission [21]. Copyright 2023, Wolters Kluwer Health.

2.3. Prediction of cancer recurrence risk

Ten to fifteen percent of individuals with BRCA are predicted to have a recurrence within five years of their diagnosis [84]. At the moment, clinical guidelines support MammaPrint (a 70-gene assay) and Oncotype DX (a 21-gene assay) for predicting the risk of recurrence [52,85]. Both of these tests are important for deciding on treatment options [86], such as whether chemotherapy is needed. But these techniques possess certain limitations. Their elevated cost restricts their extensive utilization. Oncotype DX is most helpful for patients with hormone receptor-positive, HER2-negative, and lymph node-negative BRCA, whereas its prognostic value diminishes for other subtypes, including HER2-positive or TNBCs. MammaPrint necessitates sophisticated laboratory apparatus and proficient specialists, imposing stringent requirements on both the testing environment and human credentials. Advancements in AI present a significant opportunity for creating more universally applicable and cost-efficient systems that may reliably forecast recurrence, thereby enhancing patient outcomes.

Yu *et al.*'s study looked at the association between MRI characteristics and long non-coding RNAs (lncRNAs) and used DL radiomics to predict RFS in patients with BRCA based on MRI data [26]. This research introduced a model called Radiomic DeepSurv Net (RDeepNet) (Fig. 5A), which utilizes the DeepSurv deep neural network (DNN) and Cox proportional hazards to forecast the recurrence risk for individual patients. The RDeepNet model's originality is in its capacity to amalgamate radiomic information from the tumor and adjacent tissue, together with data from contrast-enhanced T1-weighted imaging (T1 + C) and T2-weighted imaging (T2WI) sequences. The research examined data from 1113 individuals with non-metastatic IBC, categorized into training, validation, and test cohorts. RNA sequencing was conducted to examine the relationship between radiomic characteristics and the tumor microenvironment (TME). In the training cohort, RDeepNet demonstrated exceptional prediction accuracy, with AUC of 0.98, 0.94, and 0.92 for 1-, 2-, and 3-year RFS, respectively. Survival analysis was conducted utilizing the Kaplan-Meier technique and log-rank test, while HR and 95 % CI were computed by Cox regression, therefore validating the model's strong predictive efficacy. The model exhibited robust generalization across diverse molecular subtypes and patient cohorts undergoing varied therapies, indicating that RDeepNet had extensive clinical application. This signifies that the approach is applicable to a diverse array of BRCA patients, providing individualized forecasts of recurrence risk. Additionally, it highlights how radiomics may be used to non-invasively measure lncRNAs, providing a fresh viewpoint for therapy choices.

In multicenter research, Han *et al.* investigated the utilization of DL in medical image analysis by integrating ultrasound (US) and mammography (MG) pictures with clinical data to enhance prediction accuracy [27]. The research employed a ResNet50-based deep learning model (DLM) (Fig. 5B), including distinct models for US (US DLM), MG (MG DLM), and a unified model (US + MG DLM). A clinical model and an integrated model were also created, the latter of which combined the US + MG DLM with independent prognostic variables. The combined model attained an AUC of 0.882 in the training set and 0.739 in the test set, demonstrating robust predictive efficacy. The efficacy of this model is ascribed to its amalgamation of US and MG images, in conjunction with patho-

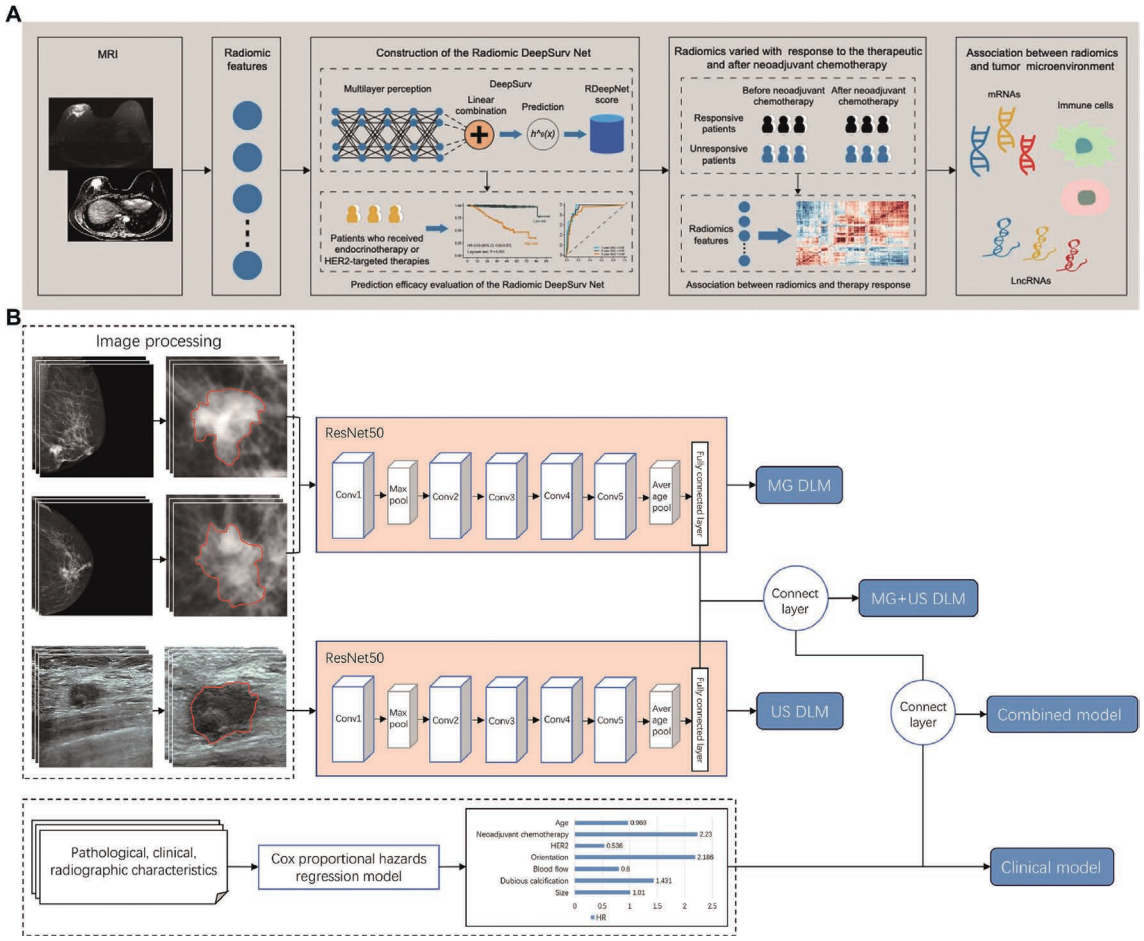


Fig. 5. Representative AI Models for BRCA recurrence risk prediction. (A) The deep-learning-based Radiomic DeepSurv Net was constructed with MRI radiomic features, and was found to be employed for RFS prediction and associated with therapy response and TME. Reproduced with permission [26]. Copyright 2023, Springer Nature. (B) Establishment of DLMs based on ResNet50. Reproduced with permission [27]. Copyright 2024, Elsevier Inc.

logical, clinical, and radiological data, which may elucidate its enhanced predictive capacity relative to single-modality models. The US + MG DLM surpassed the individual US DLM and MG DLM in both training and test cohorts, indicating that the integration of multimodal imaging data improves the model's predictive capability.

By precisely measuring lymphovascular invasion (LVI) prior to surgery, Xu *et al.* aimed to improve the prognosis of IBC [28]. LVI is a critical component in the metastatic progression of IBC [87,88], and its presence elevates the likelihood of ALN metastases and tumor recurrence in IBC patients [89–91]. The study created and validated a ML model that incorporates clinical and MRI variables to assess the preoperative LVI status and examines its correlation with DFS. The researchers utilized many ML methods, such as LR, XGBoost, k-nearest neighbors (KNN), and SVM, integrating clinical and MRI data to construct the models. The findings demonstrated that the XGBoost-based model surpassed the others in both training and validation datasets, attaining AUC values of 0.832 and 0.838, respectively. The LVI score produced by the XGBoost model was identified as an independent predictor of DFS (adjusted HR: 2.66). This validated the enhanced predictive capability of the XGBoost model, presumably attributable to its ensemble structure based on DT, which integrates supplementary regularization techniques to control model complexity and avert overfitting, resulting in improved accuracy during initial training. The XGBoost model's predictions demonstrated that a high LVI score is strongly linked to shorter DFS, suggesting that the presence of LVI corresponds with a worse prognosis in IBC patients. In addition to offering more proof of the link between prognosis and LVI, the study emphasizes the XGBoost model's possible therapeutic utility in predicting outcomes and evaluating LVI prior to surgery in IBC patients. This ML technique enables doctors to assess a patient's LVI condition with more precision, facilitating more tailored treatment regimens.

3. Utilization of AI in treatment plan selection

The stratification of recurrence risk by AI models, as detailed in Section 2.3, provides the critical foundation for personalized therapeutic decision-making. Patients identified as high-risk typically require more intensive interventions, whereas low-risk cohorts may benefit from de-escalated therapies to minimize unnecessary toxicity. Building upon these predictive insights, AI systems now extend their utility to optimizing treatment selection through three capabilities: Forecasting therapeutic responses prior to intervention, dynamically evaluating treatment efficacy during clinical course, and identifying optimal therapeutic combinations. This shift from risk prediction to intervention optimization represents a cornerstone of precision oncology in BRCA management. Table S2 (Supporting information) summarizes the rapidly evolving landscape of AI applications in this domain. In neoadjuvant therapy, conventional prediction methods predominantly depend on single-modality imaging evaluations, including morphological characteristics observed in ultrasound or mammography, or a restricted array of clinical-pathological factors, such as hormone re-

ceptor status and tumor grading. These techniques have obvious drawbacks, such as fragmented modality information, poor dynamic change capture, and a limited ability to assess the heterogeneity of the tumor microenvironment. These issues have been greatly resolved by AI algorithms that integrate multi-modal input and extract characteristics in great detail. Using end-to-end DL architectures, AI integrates data from several modalities to find non-linear correlations in complicated datasets [8,92]. The ability of AI models to identify early markers of treatment response from time-series data, enables predictions of treatment success before or soon after the start of treatment, offering a crucial window for dynamic therapy modifications. Additionally, by employing explainable methods (such as feature contribution analysis and attention processes), AI helps physicians comprehend the reasoning behind model decisions by revealing the biological significance of important predictive features. In contrast, such mechanistic insights are difficult to uncover using standard approaches that rely on human feature engineering. Aside from improving prediction accuracy, these advantages allow AI to change the paradigm from population-based treatment to individualized dynamic decision-making. The AI-driven LightGBM ML model, created by Li *et al.* [93], employs a blend of preprocessed and first-contrast-enhanced T1-weighted imaging (T1WI) radiomic characteristics (Fig. 6A). This model has outstanding efficacy in predicting pathological complete response (pCR) after neoadjuvant treatment for BRCA, with an AUC of 0.823, an accuracy of 74.0 %, a sensitivity of 85.0 %, and a specificity of 67.2 %. LightGBM is esteemed for its superior accuracy, stability, and capacity to manage extensive datasets, in addition to its rapid training capabilities. The non-invasive early prediction of pCR can aid doctors in refining treatment strategies, minimizing needless medication toxicity, and averting disease progression. Other clinical scenarios, such as forecasting pCR, analyzing patient reactions to various therapies, and evaluating therapeutic results, also use AI models. The amalgamation of several imaging modalities, such as MRI, ultrasound, and digital breast tomosynthesis (DBT), with AI has significantly improved predicted accuracy. Certain models can predict treatment-related toxicities, facilitating the identification of patients most suited for certain medicines. In the optimization of treatment strategies, DL algorithms are employed in high-dose-rate brachytherapy to forecast dosage distribution, thereby improving the efficiency and accuracy of dose computation. Multi-task DL models may be utilized to customize radiation therapy programs for specific patients in partial breast irradiation. ML and DL models are essential in enhancing several facets of radiotherapy, such as post-operative intensity-modulated radiation treatment (IMRT), automated segmentation, quality assurance (QA) predictions, and clinical surface-guided radiation therapy. Also, DL is progressively utilized in breast-conserving surgery for functions like tumor segmentation, surgical navigation, margin evaluation, and surgical planning, all of which enhance surgical precision and success rates.

3.1. Forecasting and assessment of treatment efficacy

AI models demonstrate significant scalability and are utilized across multiple areas of neoadjuvant therapies, such as NAC, radiotherapy, systemic therapy, and targeted therapies. Analysis of extensive clinical, imaging, and genetic data from BRCA patients enables AI models to identify patterns and features associated with treatment response and effectiveness. This facilitates the timely prediction of treatment outcomes and precise evaluations of therapeutic efficacy. This document will classify AI models into distinct categories according to their data sources.

AI models employing the RF algorithm have demonstrated the ability to predict pCR in HER2-positive BRCA patients within the framework of NAC by examining their clinical characteristics [97]. These models identify critical clinical parameters, including estrogen receptor (ER) status, progesterone receptor (Pgr) status, and HER2 scores, that are significantly correlated with pCR, demonstrating adequate predictive performance (AUC of 73.27 % and accuracy of 71.67 %). Relying solely on clinical characteristics is inadequate for developing a clinically effective decision support system.

The integration of AI with medical imaging technology presents considerable potential. Recent studies indicate that MRI-based radiomics, in conjunction with AI, can effectively predict the efficacy of NAC. Multimodal MRI radiomic models extract features from various MRI sequences, such as T1-weighted imaging, T2-weighted imaging, and dynamic contrast-enhanced MRI (DCE-MRI), to obtain a comprehensive understanding of tumor characteristics (Fig. 6B) [94]. In contrast, multi-region MRI radiomic models emphasize features derived from various tumor regions, including the tumor interior, adjacent tissue, and background parenchymal enhancement (BPE) areas (Fig. 6C). These models examine the impact of the TME on the response to NAC, focusing specifically on the BPE region, which may be associated with tumor growth and metastasis [95]. Integrating features from various regions enhances the comprehension of the tumor's biological characteristics. An AI system that integrates multi-region DCE-MRI and clinical pathological data (Fully automated integrated system based on deep learning, FAIS-DL) incorporates multi-region DCE-MRI features alongside critical clinical factors, including tumor size, lymph node status, and hormone receptor status. This system employs DL methods to autonomously segment the tumor and lymph nodes (Fig. 6D) and forecasts axillary pCR [96]. In the pooled external and prospective test sets, the FAIS-DL decreased the unnecessary axillary lymph node dissection rate from 47.9 % to 6.8 %, and increased the benefit rate from 52.2 % to 86.5 %. FAIS-DL is anticipated to provide enhanced predictive accuracy for pCR when compared to the prior two models, owing to its comprehensive methodology. The integration of multi-region DCE-MRI features with clinical pathological information provides a comprehensive understanding of the tumor's biological characteristics. DL significantly enhances the model's capacity to identify intricate patterns, thereby improving prediction accuracy. The automation offered by FAIS-DL diminishes human bias and enhances its applicability in clinical environments.

Ultrasound imaging offers real-time two-dimensional or three-dimensional visualizations and can be integrated with techniques such as elastography to evaluate tumor stiffness and morphology. Ultrasound images, when integrated with AI algorithms for comprehensive analysis, can facilitate accurate predictions of chemotherapy response. Falou *et al.*'s work used transfer learning to predict how locally advanced breast cancer (LABC) will react to NAC before treatment by using quantitative ultrasound (QUS) imaging [98]. The research utilized the ResNet DL architecture to extract features from parametric QUS images, employing SelectKBest and SMOTE techniques for feature selection and data balancing. The SVM algorithm was utilized to categorize patients as non-responders (NR) or responders (RR). The model exhibited notable performance on an unseen test set, particularly with spectral slope parameter maps, achieving an accuracy of 100 %, a recall of 71 %, an F1 score of 83 %, and a balanced accuracy of 86 %. In a different research project, Gu *et al.* created two multimodal ultrasound DL models based on Densenet121 networks [99], DL_Clinical_PCR and DL_Clinical_resistance, to predict pCR and resistance to NAC, respectively. The models integrated grayscale two-dimensional ultrasound, elastography, and essential clinical-pathological data, including ER, HER2, and tumor volume. DL_Clinical_resistance demonstrated an AUC of 0.911 and a sensitivity of 0.905 in the test cohort. In contrast, DL_Clinical_PCR exhibited an AUC of 0.880, with sensitivity and NPV recorded at 0.875 and 0.895, respectively. The integration of both models in the study identified 37.1 % of patients with resistance and

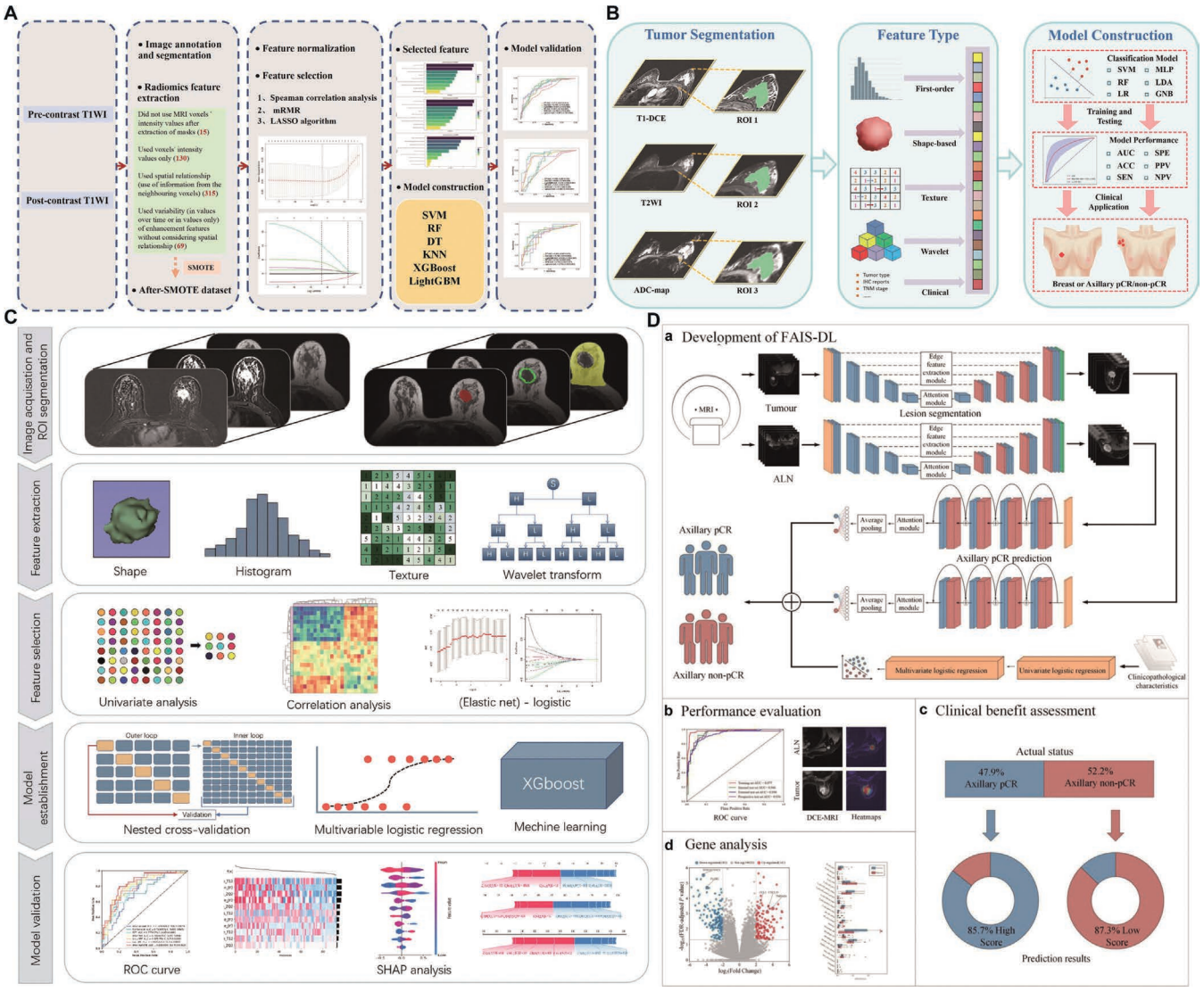


Fig. 6. Representative AI models for BRCA treatment response prediction and effectiveness evaluation. (A) Flowchart of the radiomics-based predictive model construction for pathologic complete response to NAC in BRCA. Reproduced with permission [93]. Copyright 2024, The Authors. (B) Workflow diagram of predicting NAC response based on multi-parametric MRI radiomics models. Reproduced with permission [94]. Copyright 2024, Elsevier Ltd. (C) Flowchart of multi-region MRI radiomics feature extraction and ML model construction. Reproduced with permission [95]. Copyright 2024, Springer Nature. (D) Development workflow of multi-regional dynamic contrast-enhanced MRI DL models. Reproduced with permission [96]. Copyright 2024, Elsevier B.V.

25.7 % with pCR, indicating that these patients may benefit from early modifications to treatment plans or organ-preserving strategies following NAC. These studies indicate that the QUS model predominantly forecasts NR to NAC, while the multimodal ultrasound model predicts both resistance and PCR outcomes. The multimodal ultrasound model potentially provides enhanced predictive performance for NAC responses by integrating grayscale ultrasound and elastography, thereby offering a more comprehensive array of tumor characteristics [100], which improves prediction accuracy. Incorporating essential clinical-pathological information into the final fully connected layer likely enhances the multimodal ultrasound model's capacity to address tumor heterogeneity [101], thereby improving prediction accuracy. The Densenet121 network enhances feature transmission efficiency *via* dense connections, potentially facilitating more effective learning and improved generalization of the model. When selecting the optimal model for real-world applications, it is essential to consider factors such as data availability, computational cost, and clinical feasibility.

Conventional DBT imaging, when combined with AI models, has considerable potential for forecasting pCR in BRCA patients receiving NAC. In an innovative work by Fornvik *et al.* [102], DL methodologies were utilized on continuous DBT photos. This study assessed DBT pictures both before NAC and after two and six cycles of chemotherapy, offering a full assessment of the tumor's response throughout time. The AI model employed a 3D ResNet as the foundational network for feature extraction and included advanced attention and prediction modules [103], allowing the machine to concentrate more efficiently on essential elements within the pictures. This method achieved a strong predictive performance on the test set, evidenced by an AUC of 0.83. The study utilized GradCAM to provide a visual elucidation of the model's decision-making process, hence augmenting the transparency and reliability of AI in medical applications [104,105]. Xing *et al.* concentrated on the under-researched ER+/HER2- BRCA subtype [106], which is treated with NAC. They devised a DL model utilizing contrast-enhanced spectral mammography (CESM) and integrated it with clinical and pathological characteristics to formulate a nomogram

for predicting NAC response, therefore enhancing the clinical usefulness and interpretability of the findings. ER+/HER2- BRCA frequently encounters treatment resistance challenges, including resistance to CDK4/6 inhibitors due to Rb loss or ESR1 mutations. A recent review summarized advancements in combination therapies for ER-positive BRCA, highlighting that the cross-talk between ER and pathways such as phosphatidylinositol 3-kinase/protein kinase b/mammalian target of rapamycin (PI3K/AKT/mTOR) and Histone Deacetylase (HDAC) plays a pivotal role in resistance development. Furthermore, multi-target combination strategies (*e.g.*, combining Selective Estrogen Receptor Degraders (SERDs) with HDAC inhibitors) have shown promise in delaying resistance. This clinical need underscores the potential of AI models to predict resistance risks and optimize combination therapy plans through the integration of multi-omics data [30].

The promise of AI also encompasses the examination of digital pathological pictures. A unique, multi-layered, self-attention-guided DL framework has been created to interpret digital pathology pictures from preoperative tumor samples, facilitating early prediction of treatment response [107]. This structure incorporates processing modules at three tiers: Local, tumor, and patient. It integrates convolutional layers with self-attention processes, enabling the model to proficiently assess both local characteristics and global relationships in pathological pictures. The layered processing technique effectively tackles the issue of training DL models on high-resolution whole-slide images (WSIs) that are often limited by memory constraints. PROACTING, a DL-based computational biomarker created by Aswolinskiy *et al.* [108], forecasts reactions to NAC by examining standard H&E-stained pathology slides. The innovation resides in its capacity to discern critical elements within the TME, including tumor cells, lymphocytes, and stroma, while quantifying biomarkers linked to pCR, such as lymphocyte-to-tumor ratio (LTR), the ratio of inflammatory tumor to total tumor volume (ITR), tumor-infiltrating lymphocyte score (cTILs), and mitotic rate. This model has demonstrated potential in predicting pCR across many datasets, with AUC values between 0.66 and 0.88. This indicates that AI may diminish overtreatment, enhance treatment techniques, and augment the capacity to identify individuals likely to react to chemotherapy in clinical environments.

Within the framework of neoadjuvant radiation (NART), the SuperTIL model [109], which incorporates DL analyses at cellular and tissue levels, has demonstrated significant concordance with manual assessments. Through a longitudinal analysis of tumor samples from patients with BRCA in the PRADA and Neo-RT clinical trials, the research team found that the SuperTIL score closely matched the pathologists' manual evaluation of stromal tumor-infiltrating lymphocytes (sTILs) ($P < 0.0001$). SuperTIL's predictive performance (AUC = 0.79) was comparable to manual scoring (AUC = 0.79) in predicting pCR, and its combined model (AUC = 0.80) significantly improved prediction accuracy. Moreover, SuperTIL demonstrated superior efficacy in differentiating between high- and low- sTIL groups. Other cellular-level scores, such as cTIL, were more impacted by changes in threshold values than their tissue region-based lymphocyte density score, which measures the proportion of lymphocytes in the stroma to the stromal area. As a result, the SuperTIL model has great potential for application in clinical practice and not only validates the clinical usefulness of manual scoring but also provides new technological assistance for planning clinical trials that combine immunotherapy and radiotherapy, especially in terms of improving patient stratification and efficacy prediction.

The balanced individual treatment effect for survival (BITES) data model [110]is a semi-parametric survival regression DL model developed for neoadjuvant systemic treatment (NST) [110,111]. Through the equilibrium of treatment group distributions and the utilization of shared and risk networks to compute individualized treatment effects [112], statistically significant protective outcomes have been evidenced, including a reduction in BRCA mortality and an extension of patient survival exceeding 21 months, following adjustments for baseline characteristics *via* inverse probability treatment weighting (IPTW). This model demonstrates the capabilities of DL in customized medicine and provides accurate clinical treatment recommendations, enhancing individualized medical strategies for BRCA patients. On the basis of nonlinear mixed-effects modeling and ML algorithms, research has created a predictive model that quantifies differences in animal survival rates and metastatic dynamics and finds important biomarkers for predicting metastatic potential [113]. This model replicates the inhibition of primary tumor development and the prevention of postoperative metastatic progression by neoadjuvant receptor tyrosine kinase inhibitor therapies, serving as a tool for improving NAT planning and predicting treatment results.

AI has proven to be highly effective in predicting treatment outcomes and assessing therapeutic benefits outside of NAT. A radiomics feature model utilizing ML can forecast the TME phenotype and the response to immunotherapy in BRCA patients by evaluating DCE-MRI and RNA sequencing data [114]. The BITES model innovatively integrates meta-learning and latent representation-balanced causal inference strategies [111], providing personalized adjuvant chemotherapy recommendations and accurately predicting treatment outcomes for elderly BRCA patients while also identifying treatment heterogeneity [115]. Moreover, combining ML with urban features has enhanced the model's applicability across different populations [116]. A DL algorithm, DeepTEPP [117], utilizing preoperative breast MRI, may non-invasively forecast the response of HER2-positive BRCA patients to anti-HER2 therapy, hence assisting in the customization of treatment strategies. A novel ML prognostic model centered on palmitoylation-related genes utilizes the "limma" package to identify differentially expressed genes [118,119], the "WGCNA" package for creating gene networks, and least absolute shrinkage and selection operator (LASSO) Cox regression to develop a prognostic model [120,121]. This model, in conjunction with the "regplot" software [122], generates a nomogram for forecasting patient survival and their reactions to chemotherapy and immunotherapy. Not only can CTRGPS, a predictive signature based on genes associated with $CD8^+$ T cells [123], increase the precision of early diagnosis and therapy for BRCA, but it also reveals TTK protein kinase (TTK) as a potential target for treatment. Utilizing bioinformatics and ML to find biomarkers linked to $CD8^+$ T cells in order to forecast clinical outcomes and treatment responses in patients with BRCA [124], one study demonstrated the crucial role that $CD8^+$ T cells play in slowing the growth of BRCA. An AI model employing adaptive LASSO algorithms may use metabolomics to forecast probable neuro- and metabolic toxicities post-BRCA therapy [125], assisting physicians in formulating more effective treatment strategies and reducing unwanted toxic consequences. In early-stage BRCA patients receiving accelerated partial breast irradiation (APBI), a multivariable LR model can assist doctors in identifying individuals most likely to benefit from OART [126], hence improving treatment allocation prior to the commencement of therapy.

3.2. Enhancement of therapeutic approach

Conventional clinical methodologies depend heavily on average data from populations, which frequently neglect the need for individualized care. The use of AI technology in BRCA therapy is becoming an essential instrument for enhancing therapeutic tactics. High-dose-rate (HDR) brachytherapy is a radiation method in which a highly radioactive source, usually iridium-192, is temporarily implanted into the patient's body to directly irradiate the tumor [127]. This approach is regarded as an efficacious localized

therapy, as it administers a concentrated radiation dosage directly to the malignant cells. The precision of dose estimation in HDR brachytherapy is crucial for both effective treatment and the reduction of inadvertent harm to adjacent healthy tissue. Conventional dose estimation approaches, such as the TG-43 formula [128], neglect the impact of tissue heterogeneity in patients. Conversely, the monte carlo (MC) simulation rectifies these deficiencies by providing more accurate dosage distributions [129]. Despite this, MC simulations are computationally demanding and time-consuming [129], accordingly restricting their practical application in clinical environments. Quetin and colleagues investigated the application of DL methodologies to forecast high-resolution dose distributions for HDR brachytherapy in BRCA treatment [130]. They evaluated two models: 3D U-Net and the combining network (C-Net). The 3D U-Net, employed as a baseline model, forecasts dosage maps by extracting characteristics *via* downsampling and upsampling layers. Simultaneously, C-Net employs two distinct CNNs to encode individual input characteristics, which are subsequently amalgamated to produce a cohesive output volume. The U-Net-D5 model excelled at predicting voxel doses; however, the C-Net-D5+ model demonstrated superior robustness in forecasting dose metrics, with a mean absolute percentage error (MAPE) of less than 1.1 % across all dosage indicators. Both models showed remarkable efficacy in forecasting dose distributions, nearly aligning with MC simulations while achieving a 300-fold improvement in speed, so rendering rapid and precise dosage computations viable for practical use. Simultaneously, Moore *et al.* improved BRCA treatment through enhanced dose prediction accuracy and the automation of radiation planning [131]. They created a 3D dosage prediction model that integrates a "luminescent" masking technique with a gradient-weighted mean squared error (GW-MSE) loss function (Fig. 7A). The model achieved a mean ME of 0.40 %, mean absolute error of 2.70 %, an error in mean dose to heart and lung of −0.10 and 0.01 Gy, and an error in mean dose to the tumor bed of −0.01 %. This advanced approach attains high-precision dose estimates utilizing just CT scans and the contours of three essential organs (tumor bed, heart, and contralateral lung) as input, hence obviating the necessity for manual contouring or planned target volumes (PTVs). This method markedly enhances the automation of treatment planning, diminishing variability in treatment plans and augmenting overall efficiency.

APBI has become more favored in the management of early-stage BRCA owing to its precise dosage administration and reduced treatment time. However, since APBI may be applied in a variety of ways, it can be difficult to determine the best dosage administration strategy for each patient's particular requirements. In response, Maniscalco *et al.* created a multi-task DL model to tailor the choice of the most effective radiation treatment for APBI [136]. The model employs two CNNs based on DL: a single-task (ST) network that forecasts the dosage for one technique and a multi-task (MT) network capable of concurrently predicting the dose distribution across several treatment modalities. Their findings indicated that while the MT model necessitated a longer training duration than the ST model, it demonstrated more efficiency in forecasting the treatment time necessary for each patient (1.82 s *vs.* 0.93 s). Moreover, the MT model demonstrated superior performance compared to the ST model, as evidenced by a lower MAPE across all patients (1.1033 % ± 0.3627 % *vs.* 1.2386 % ± 0.3872 %), which suggests more precise predictions. This model's originality is in its capacity to concurrently forecast various dosage distributions. Through the sharing of encoder and decoder layers, the model enhances its generalizability and mitigates overfitting, thereby establishing a scalable and adaptable framework that can facilitate resource optimization and personalized dosage prediction in clinical decision-making. In addition, AI technology has been applied to other aspects of radiotherapy optimization, such as the prediction of the optimal number of irradiation fields in IMRT for BRCA using RF-ML models [137]. This has improved the efficiency and accuracy of radiotherapy planning. AutoContour is a DL-based automatic segmentation model (Fig. 7B) that offers geometric and dosimetric precision for breast-conserving and regional lymph node structures in BRCA radiotherapy plans [132], comparable to manual segmentation performed by physicians, although additional refinement is required for certain structures, including internal mammary nodes. To forecast the QA outcomes of BRCA IMRT treatment plans with exceptional accuracy, a novel DL model (Fig. 7C) has been created to examine complexity indicators unique to the Halcyon system. This markedly improves the efficiency and accuracy of patient-specific QA in radiotherapy with an AUC of 0.95, specificity of 0.98, and sensitivity of 0.97 [133]. Additionally, ML technologies may be used in conjunction with clinical surface-guided radiation treatment (SGRT) [134], utilizing synthetic human body datasets and DL models like MobileNet-v2 to detect important anatomical landmarks (Fig. 7D). The aROIbreast algorithm demonstrated superior performance in compliance with institutional protocols, achieving a DSC of 0.83 ± 0.04, a quality score of 8.2 ± 0.9, and an acceptance rate of 14.6/15. Notably, the automated creation of ROIs was markedly expedited, with the aROIbody and aROIbreast algorithms requiring only 1.3 s and 1.2 s, respectively. This is a significant reduction compared to the approximately 120 s needed for manual cROI creation, leading to a considerable enhancement in workflow efficiency.

The primary obstacle in breast-conserving surgery (BCS) is the complete removal of the tumor without the presence of positive margins, a factor that makes a substantial contribution to cancer recurrence. The prevalence of positive margins in BCS is around 20 % [138], which raises healthcare costs and worsens patient discomfort. Researchers are therefore in pursuit of technological innovations that will enhance the precision and effectiveness of surgical procedures. In an effort to automate the contouring of tumors and direct their excision in real time, DL, which is recognized for its adeptness in image recognition and segmentation, has been integrated into surgical navigation and tumor delineation. Despite several drawbacks in clinical margin prediction, Yeung *et al.* found that the nnU-Net model was the most successful for breast ultrasonography tumor segmentation [139]. It was noteworthy for its automated and effective tumor contour construction. Its excellent ranking in expert visual ratings and good quantitative performance yet demonstrate how DL may improve breast surgery precision. Additionally, the necessity for multiple surgeries can be significantly reduced by assessing surgical margins during breast-conserving surgery for BRCA. By utilizing the swin transformer DL model (Fig. 7E) and dynamic full-field optical coherence tomography (D-FFOCT) [140], Zhang *et al.* created an intraoperative cancer detection procedure that allows for near real-time [135], non-destructive automated BRCA diagnosis. The model yielded excellent performance, with an accuracy of 97.62 %, sensitivity of 96.88 % and specificity of 100 %; only one IDC was misclassified. This method greatly improves intraoperative diagnostic accuracy and efficiency by combining high-resolution optical imaging with advanced computer vision algorithms. When patients are in the supine position for surgery, the position of breast tumors as seen in MRI scans can migrate, resulting in significant breast deformation and obstructing accurate tumor localization. This can occur during actual surgical procedures. In response to this issue, Dolega-Kozierowski *et al.* developed a DNN-based AI model that integrates MRI with three-dimensional scanning data [141]. This model simulates the displacement of breast tissue and tumors under various positions, providing a novel, high-precision predictive tool for surgical planning in BRCA patients. Furthermore, the addition of 3D-printed transparent breast models to surgical procedures offers a visually intuitive aid.

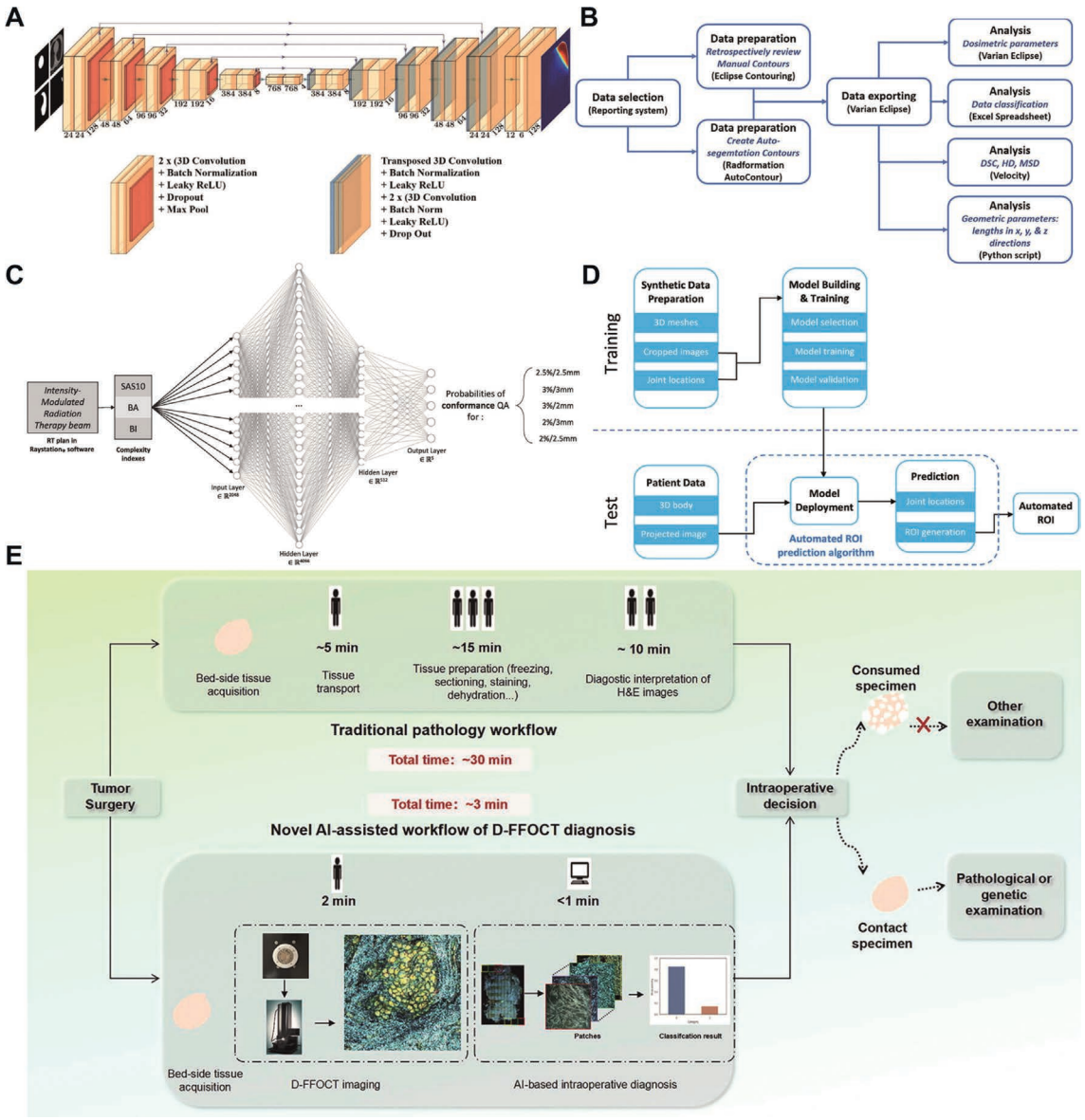


Fig. 7. Representative AI models for treatment strategy optimization. (A) 3D U-Net model architecture for dose prediction in breast radiotherapy. Reproduced with permission [131]. Copyright 2024, American Association of Physicists in Medicine. (B) Overall study workflow for auto-segmentation evaluation. Reproduced with permission [132]. Copyright 2024, Wiley Periodicals LLC. (C) DL model architecture for halcyon QA prediction. Reproduced with permission [133]. Copyright 2024, Elsevier B.V. (D) Flowchart of the automated ROI selection algorithm based on body contour (aROIbody). Reproduced with permission [134]. Copyright 2023, Wiley Periodicals LLC. (E) Comparison of intraoperative diagnosis workflows for conventional H&E-based histology and D-FFOCT plus DL. Reproduced with permission [135]. Copyright 2024, Elsevier B.V. and Science China Press.

4. AI-assisted drug development

AI significantly contributes to BRCA prediction and diagnosis by providing essential insights and multidimensional data that facilitate drug discovery. The integration of diverse data sources, including pathology, radiomics, and genomes, enables AI models to precisely categorize patient groups and detect important molecular characteristics, such as HRD deficiencies and HER2-low status. These models reveal fundamental pathogenic mechanisms and identify potential therapeutic targets within biological networks. Furthermore, the correlation between radiomic properties and the features of the tumor microenvironment discovered by AI-based radiomics models can aid in the reversal of crucial signaling pathways. Potential medication inhibitors can then be quickly screened using virtual chemical libraries created by DL algorithms. The process of repurposing existing medications can also be accelerated by integrating knowledge graphs with drug target databases and AI-based prognostic models (like the RDeepNet model, which links lncRNAs). This closed-loop system, driven by data, ensures that biomarkers identified in disease prediction are directly applicable to drug development. It optimizes clinical trial designs by selecting appropriate patient populations through predictive models, utilizes digital biomarkers from pathology images to monitor drug responses, and ultimately establishes a translational medicine pathway from accurate diagnosis to targeted treatment.

AI-assisted drug development represents a revolutionary paradigm shift in the pharmaceutical field, leveraging AI to fundamentally enhance the precision and efficiency of research and development. By integrating advanced computational tools with extensive biological and chemical datasets, AI significantly accelerates the initial stages of drug discovery. This integration empowers researchers to rapidly screen, identify, and optimize potential

drug candidates, streamlining the early phases of pharmaceutical development.

A cornerstone of AI's utility in drug development is its proficiency in analyzing extensive chemical compound libraries to pinpoint those with the highest potential for interacting effectively with specific disease targets, thereby drastically reducing the time and costs traditionally associated with drug discovery. Moreover, AI significantly enhances the design of novel molecular entities by predicting their structural properties, binding affinities, and therapeutic effects. For instance, AI can evaluate the efficacy of new compounds against specific targets, such as BRCA-related genes, by simulating their molecular interactions. This predictive power not only optimizes the drug discovery pipeline but also increases the likelihood of identifying safe and effective drugs more swiftly [142,143]. This shift toward AI-driven drug discovery is transforming the pharmaceutical industry, enabling the development of highly targeted and effective therapies for a wide range of diseases, including cancer, genetic disorders, and infectious diseases. The AI models developed in this area are compiled in Table S3 (Supporting information).

4.1. AI-assisted target identification in BRCA

AI is increasingly transforming the traditional medication research and development process. AI technology can uncover important genes and signaling pathways implicated in the beginning and progression of illness by utilizing the analysis of vast amounts of biological data. This allows for the discovery of potential therapeutic targets. Zhang *et al.* [144], for example, identified eight important prognostic genes using transcriptome data from the TCGA and gene expression omnibus (GEO) databases and ten ML methods (ROC curve AUC $>$ 0.7, C-index = 0.761) before creating a risk model with independent prognostic value. They verified that linalool binds to the phosphoglycerate kinase 1 (PGK1) protein (PDB: 2×13) at the GLU-344 and PHE-343 sites with stability using molecular docking and dynamics simulations (RMSD = 1.44 Å, binding energy = −5.2 kcal/mol). Linalool significantly reduced the migration/invasion (Transwell $P < 0.05$), induced apoptosis, caused G0/G1 phase cell cycle arrest, and suppressed the proliferation of BRCA cells (half-maximal inhibitory concentration (IC_{50}) = 189.7–268.8 μmol/L) *in vitro*. It also modulated the PGK1-peroxisome proliferator-activated receptor gamma (PPARγ) signaling pathway. By demonstrating that linalool inhibits PGK1 expression, this work is the first to combine computational biology with experimental validation, providing a novel strategy for targeted treatment with natural products. A multivariable ML approach called pathway-based signature for ILC (PSILC) is intended to accurately predict patients' overall survival as well as their metastasis-free survival (Fig. 8A) [145]. It also finds 16 synthetic lethality genes that specifically lower cell survival in cell lines with high PSILC scores. These genes represent useful targets for further drug screening investigations since they are highly enriched in metabolic, Rho GTPase, and hemostasis pathways. Chen *et al.* examined prognostic genes associated with lipid metabolism in BRCA and incorporated 184 distinct combinations of nine ML methods [146], including LASSO, Ridge, and Elastic Net. By analyzing and validating datasets like TCGA-BRCA, they identified 21 pivotal genes to develop the LMPGS model. Niclosamide, one of seven interesting possibilities identified by molecular docking experiments with currently available medications, had interactions with these important genes and may have an impact on the course of the illness.

MOMLIN is a multi-modal and multi-omics ML integration framework that was first presented by Rashid *et al.* (Fig. 8B) [147]. It focuses specifically on the combined use of class-specific feature selection techniques and sparse correlation algorithms. The objective of this method is to find interpretable elements in multi-modal and multi-omics data, successfully identifying important biomarkers and network biomarkers that affect medication reactions. For example, the combination of ER-negative, hemicentin 1-collagen type v alpha 1 chain (HMCN1-COL5A1) mutation, F-box protein 2-colony stimulating factor 3 receptor (FBXO2-CSF3R) expression, and CD8 functions as a multi-modal biomarker in responders and may influence the Fms-like tyrosine kinase 3 (FLT3) signaling pathway and antimicrobial peptides. Lymph node-TP53 mutation-PON3-ENSG00000261116 lncRNA expression-HLA-E-T cell rejection work together as a multi-modal biomarker in drug-resistant instances, perhaps affecting the neurotransmitter release cycle pathway. Shrikant *et al.* investigated the discovery of shared biomarkers for ovarian and BRCA by using a model that combines network analysis and ML (Fig. 8C) [148]. They found common biomarkers in huge gene datasets by using RF and other clustering algorithms. Network centrality and pathway analysis further supported cAMP response element-binding protein 1 (CREB1) as a possible therapeutic target. Their research demonstrated that CREB1 is a potent option for a distinctive therapeutic target since it is overexpressed in BRCA and under-expressed in ovarian cancer. Inhibiting CREB1 may also improve the therapy of BRCA because it is essential for several signaling pathways.

Kováčová and associates created an AI-powered prediction model that combines information from pharmacogenomics (PGx) databases with ML tools including REVEL, MetaSVM, CADD, and MutationAssessor [150]. Using this model, the functional impact of rare nsSNVs (non-synonymous single nucleotide variations) in patients with BRCA was predicted, and the potential effects of these mutations on treatment results were evaluated. One of the most important conclusions was the strong correlation between the prognosis of BRCA and mutations in the CFTR gene. Significantly lower disease-free and overall survival rates were seen in patients with uncommon nsSNVs in CFTR, indicating that CFTR may be a viable therapeutic target and may be essential for medication metabolism or action mechanisms.

Immunogenic cell death (ICD), is a form of cell death brought on by immune cell infiltration. It can strengthen the body's immune response against the tumor and restore immune surveillance in the TME [151–155]. Accordingly, Li and their group created an AI-based model that predicts how sensitive BRCA is to different therapies by utilizing 14 immunogenic cell death-associated genes (ICD-TDGs) [156]. Research has demonstrated that down-regulating protein tyrosine phosphatase receptor type c (PTPRC) decreases $CD8^+$ T cell infiltration while concurrently increasing TNBC cells' resistance to paclitaxel. Furthermore, it increases the expression of PD-L1 and IL2, suggesting that PTPRC may change immune-suppressive pathways in the tumor microenvironment to affect drug sensitivity. PTPRC is a promising therapeutic target that presents fresh opportunities for creating plans to combat medication resistance in BRCA and, eventually, enhance patient outcomes. In order to discover TNBC cell lines that are especially susceptible to certain medications, Kaushik *et al.* created a ML model to predict drug responses in these cell lines (Fig. 8D) [149]. Notably, their investigation revealed that TNBC cell lines were significantly inhibited by six medications: panobinostat, PLX4720, lapatinib, nilotinib, selumetinib, and tantespimycin. Tanespimycin outperformed the others in terms of IC_{50} and AUC, demonstrating its strong anticancer properties. Additionally, it was shown that three important biomarkers, SET domain containing 7 (SETD7), serum response factor associated rhabdomyosarcoma antigen homolog (SRARP), and YIP1 domain family member 5 (YIPF5), play crucial roles in determining how sensitive TNBC cells are to these medications. While YIPF5 and SRARP were sensitive to both the medicines and radiation, SETD7 responded to all six medications. These results point to possible biomarkers and medication possibilities for upcoming clinical treatments for TNBC.

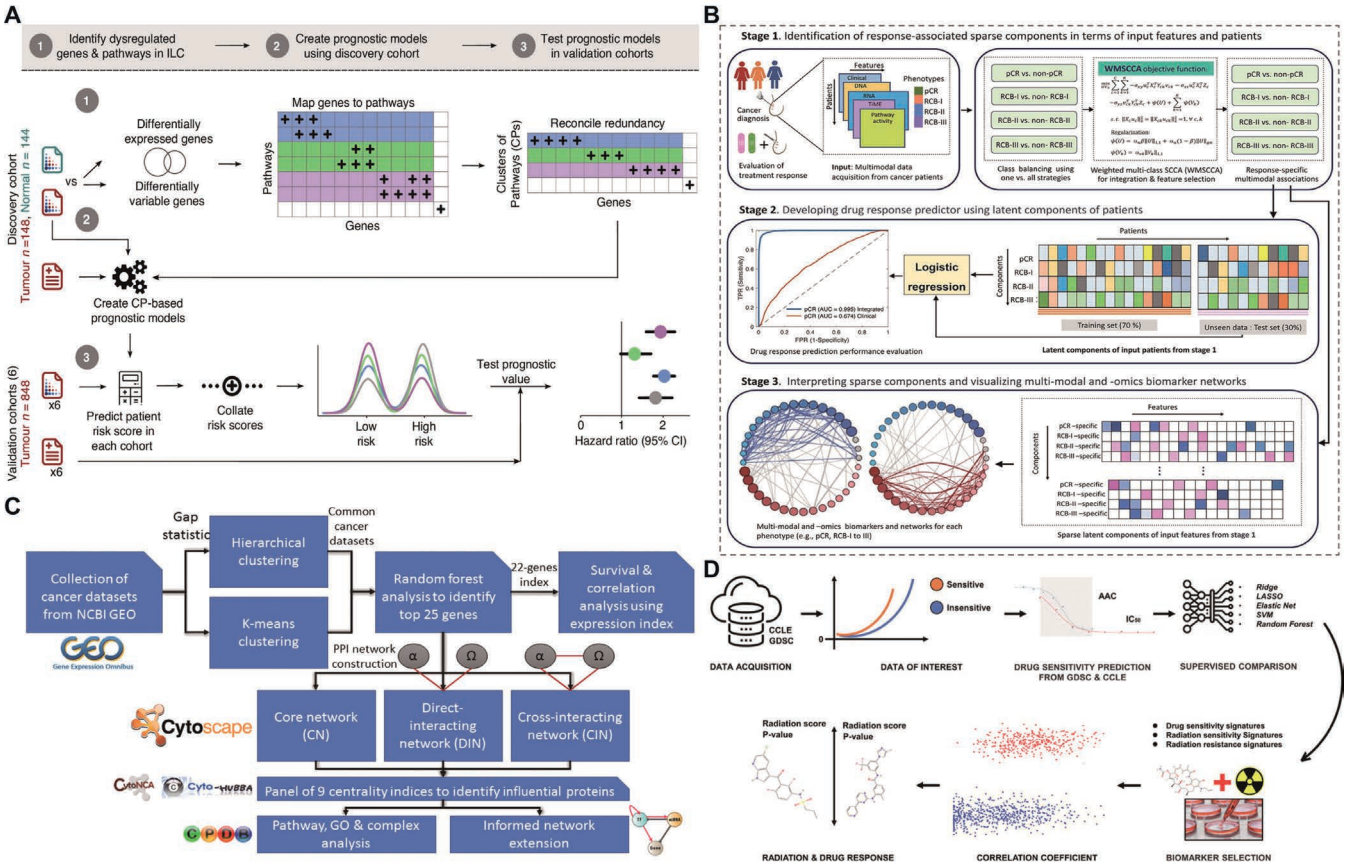


Fig. 8. Representative AI models applied to drug target development. (A) Flowchart of prognostic biomarker discovery and validation in ILC using a multivariable model. Reproduced with permission [145]. Copyright 2024, Springer Nature. (B) Flowchart of BRCA treatment response prediction using MOMLIN framework. Reproduced with permission [147]. Copyright 2024, Oxford University Press. (C) Computational analysis pipeline for identifying common cancer biomarkers of breast and ovarian types. Reproduced with permission [148]. Copyright 2020, John Wiley & Sons A/S. (D) Methodological pipeline of ML-driven exploration of drug therapies for TNBC. Reproduced with permission [149]. Copyright 2023, The Authors.

4.2. AI-assisted compound structure prediction and screening

At the forefront of modern drug discovery, AI-assisted compound structure prediction and screening technologies are leading a revolution, significantly accelerating the discovery and optimization processes of new drug candidates. In the hunt for medications to treat BRCA, AI has created new opportunities for the discovery of possible therapeutic molecules. For instance, one study developed a drug co-crystal virtual screening model using the XGBoost algorithm. This model leverages RDKit molecular descriptors (*e.g.*, HeavyAtomCount, Chi0) to predict the compatibility between active pharmaceutical ingredients and co-crystal formers. In tests with drugs like pyrazinamide, the model achieved an accuracy rate exceeding 97 %, offering a valuable methodological example for AI-assisted optimization of drug formulations in BRCA treatment (such as improving solubility) [157]. To find tiny compounds that can block miR-21 activity, Keshavarzi Arshadi *et al.* created the DL platform RiboStrike (Fig. 9A) [158]. The platform employed GCNNs to do virtual screening of nine million compounds and utilized a multi-task learning approach to elucidate the correlation between chemical groups and molecular activity from various data sources. In further tests, the candidate compounds that RiboStrike had found showed potent anti-miR-21 action and selectivity. Interestingly, one of the possibilities, Ribo21D-1, dramatically decreased the development of lung metastases in a mouse model of BRCA, indicating its possible therapeutic use and offering useful lead compounds for the creation of novel BRCA medicines.

A different research group created the Gex2SGen model (Fig. 9B) [159], which directly mapped gene expression data to SMILES representations of drug compounds using a mix of pre-trained SMILES-VAE and profile-VAE. While profile-VAE converts gene expression data to latent space, SMILES-VAE learns the structural characteristics of tiny molecules. Following collaborative training, the model may produce therapeutic compounds based on certain gene expression patterns that have the required pharmacological effects. This method has demonstrated great clinical promise in the development of drugs to treat BRCA because it can produce molecules that closely resemble known gene inhibitors like aurora kinase A (AURKA), adrenergic receptor beta 3 (ADRB3), and proteasome 20S subunit beta 5 (PSMB5), as well as compounds that are similar to well-known anti-BRCA medications like 2-methoxyestradiol, amonafide, and seliciclib. This procedure can customize treatments and expedite drug discovery, potentially enhancing efficacy and reducing side effects for BRCA patients by targeting specific gene expression patterns, while also lowering development costs and encouraging new therapies. Based on the utilization of a DL model to identify inhibitors of cancer cell cycle-dependent kinase 12 (CDK12), Wen *et al.* concentrated on using DL models to find CDK12 inhibitors [160]. They created a DTI model using the Transformer architecture, which combines a protein sequence model with a self-supervised molecular graph model (Fig. 9C). Several possible CDK12 inhibitors were effectively discovered by the model in virtual screening activities for CDK12, and these were subsequently confirmed *in vitro*. For instance, compounds CICAMPA-01, 02, and 03 had lower IC_{50} values in the HER2-positive BRCA cell line BT-474 and higher inhibitory effects in CDK12 kinase activity tests than the well-known inhibitor THZ531, providing novel candidate compounds for the development of BRCA drugs.

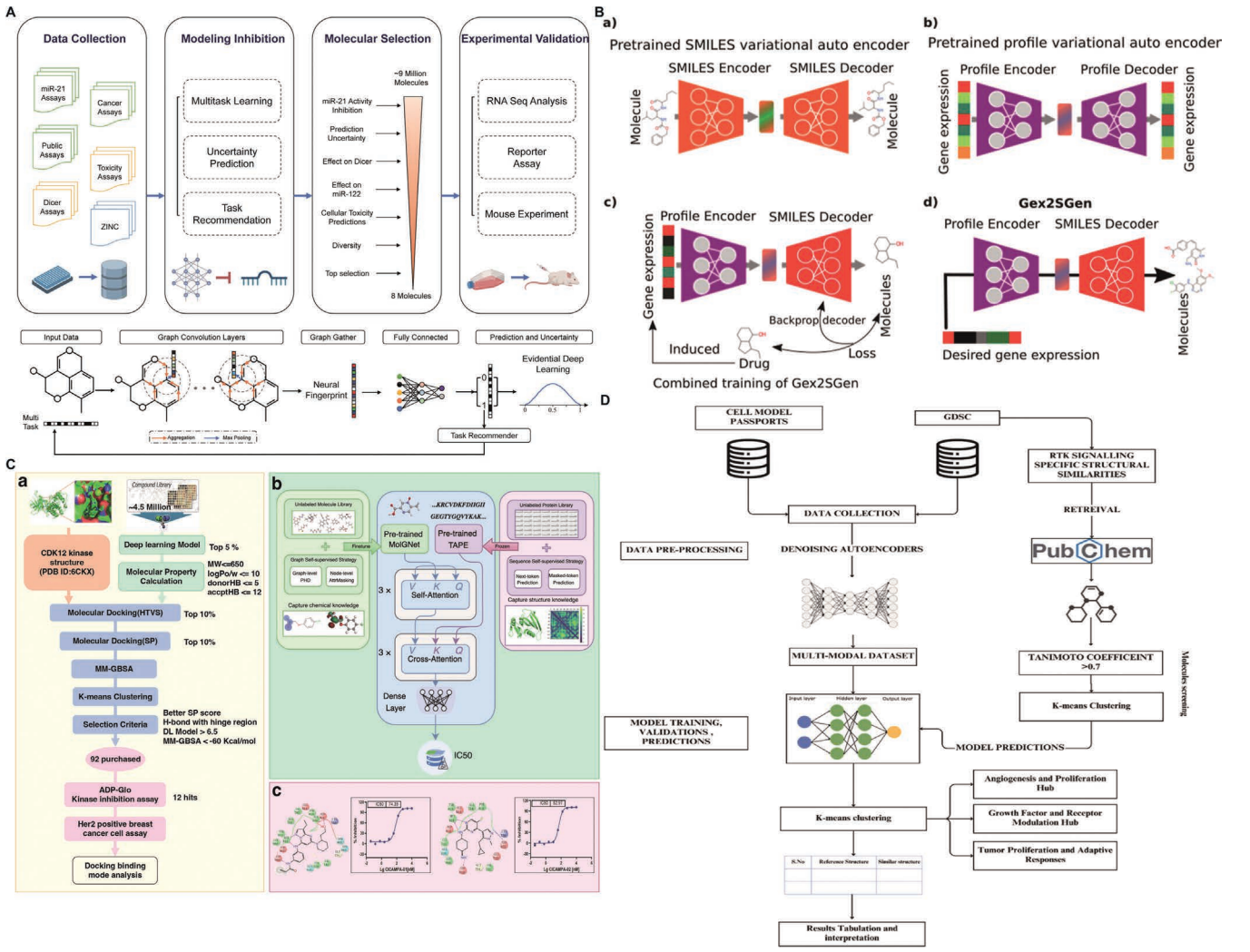


Fig. 9. AI models applied to new compound discovery. (A) RiboStrike drug discovery pipeline using GCNNs. Reproduced with permission [158]. Copyright 2023, Elsevier. (B) Gex2SGen drug design pipeline using variational autoencoders. Reproduced with permission [159]. Copyright 2023, American Chemical Society. (C) Workflow diagram of virtual screening based on DL and molecular docking. Reproduced with permission [160]. Copyright 2023, Elsevier Masson SAS. (D) Identifying novel drug candidates targeting RTK signaling. Reproduced with permission [161]. Copyright 2024, Elsevier Ltd.

Simultaneously, Karampuri *et al*. focused on finding pharmacological candidates that target receptor tyrosine kinase (RTK) signaling pathways [161]. They created a new multimodal DNN (MM-DNN)-based quantitative structure-activity relationship (QSAR) model (Fig. 9D). The novel aspect of this model is how it predicts the biological activity of medications that target the RTK signaling pathway by combining several omics data, including proteome expression data, genomic data, and drug response data. They chose RTK signaling-related pharmacological compounds from the PubChem database for their investigation, and they predicted their biological activity using the MM-DNN model. Following that, the molecules were arranged into three different clusters. The work facilitated the early phases of drug development by identifying important therapeutic candidates that target each downstream regulatory protein in the RTK signaling cascade using feature importance analysis.

4.3. AI-powered drug screening based on ADMET properties

Important aspects such as estrogen receptor alpha (ERα) function, chemical pharmacokinetics, and safety must be taken into account while researching anti-BRCA drugs. Traditional research techniques, however, are frequently expensive and time-consuming. Utilizing DL technologies to search for potential anti-BRCA medications has grown in importance as a result of their development. An AI model called ABCD-GGNN was created especially for this use [162]. Through topology, it generates atomic-level graphs and uses atomic descriptors to capture the structural and substructural characteristics of possible therapeutic options. It also selects and processes discrete molecular descriptors using XGBoost, integrating the two methods to provide molecular-level representations that can predict important pharmacological features, including ADMET qualities and ERα activity. In forecasting ERα activity and ADMET (absorption, distribution, metabolism, excretion, toxicity) characteristics, studies have shown that ABCD-GGNN works better than other models, including linear regression, RF, SVM, Bi-long short-term memory networks (LSTM), and Graph-CNN. Despite having a somewhat longer computation time, it is still within an acceptable range, which makes it a very effective tool for medication screening for BRCA. By selecting the most promising drug candidates from an existing pool, the model seeks to expedite the screening process, boost the effectiveness and success rate of drug discovery, and offer invaluable assistance and direction for future drug development.

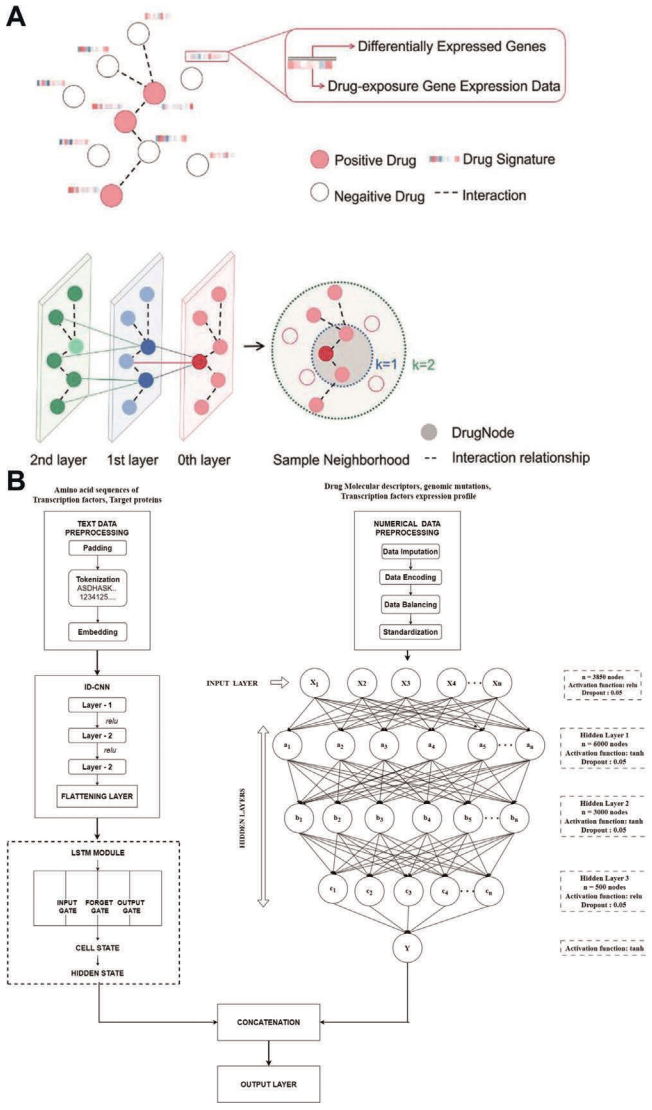


Fig. 10. AI models applied to drug repositioning. (A) Schematic of data structure and sampling-aggregation approach for drug repurposing prediction model GraphRepur. Reproduced with permission [163]. Copyright 2021, Oxford University Press. (B) Architecture of ResisenseNet model. Reproduced with permission [164]. Copyright 2024, Springer Nature.

4.4. AI-driven drug repurposing for BRCA-associated drugs

Considering how costly and time-consuming the conventional medication development process is, drug repurposing is a very beneficial strategy. To speed up the drug discovery and approval procedure, the GraphRepur model uses drug repurposing to find current medications that may be useful against BRCA (Fig. 10A) [163]. To suggest possible treatments for BRCA, this AI-based model, which is based on graph neural networks, combines drug network data with drug exposure gene expression profiles (drug signatures) and applies the GraphSAGE algorithm. It captures the topological information of drug characteristics and inter-drug connections by integrating computational approaches based on networks and signatures. This makes it an effective tool for predicting medication repurposing in BRCA. Karampuri and colleagues built a new hybrid neural network model called ResisenseNet and concentrated on comprehending drug resistance caused by transcription factors and genetic alterations (Fig. 10B) [164,165]. By merging one-dimensional convolutional neural networks (1D-CNN), LSTM, and DNN, this model efficiently integrates a variety of data sources, including transcription factor expression, genetic markers, medications, and molecular descriptors. It accurately forecasts medication sensitivity and resistance in BRCA. The originality of ResisenseNet is found in its special design, which can recognize complicated correlations in numerical data as well as long-range interdependence in temporal patterns and amino acid sequences. This offers the model exceptional precision and resilience in forecasting medication reactions, offering fresh approaches to medication repurposing and tailored treatments for BRCA. With the help of the model's predictions, 14 medications that had not yet been utilized to treat BRCA but may be sensitive to the disease were effectively repurposed from anticancer medications. These discoveries provide promise for repurposing to overcome medication resistance and open up new avenues for treating BRCA.

4.5. AI-facilitated prediction of drug synergistic interactions

Synergy generally denotes the collective impact of two or more chemicals that surpasses the anticipated results of their mere additive actions. Compared to monotherapy, drug synergy can provide far better therapeutic results, including reducing host toxicity and side effects [166], optimizing dose-effect relationships [167], and delaying the emergence of drug resistance [168,169]. Despite the fact that drug-drug synergies have been predicted and classified using ML and DL models in the past, these models are often trained on data from several forms of cancer [170], meaning they are not especially tailored for specific malignancies, like BRCA. As a result, when used on data related to BRCA, these models frequently exhibit subpar performance. Mehmood *et al.* created a particular stacked ensemble classifier model called drug-drug synergy for BRCA (DDSBC) in order to predict the cellular synergy of medication combinations that are specifically intended to treat BRCA (Fig. 11A) [171]. In terms of accuracy, precision, recall, F1 score, and AUC-ROC scores, the DDSBC model outperformed conventional models thanks to its strategic feature representation, ensemble learning, and adaptive treatment of class imbalance. This model delivers significant insights into BRCA treatment options and provides an effective approach for discovering synergistic or antagonistic medication combinations.

Paclitaxel, a chemotherapeutic medication frequently used to treat BRCA, is frequently taken into consideration for combination treatments because of its distinct mode of action and efficacy when used alone [174,175]. Using a PDX dataset and ML models, Mehmood *et al.* confirmed the efficacy of paclitaxel and various medication combinations in the treatment of BRCA [176], concentrating on the best-performing Elastic Net model. Fifty *in vivo* indicators that are strongly linked to medication response were found by the researchers. Along with offering novel biomarkers and medication combination techniques for the future of precision medicine, these discoveries also contribute to a deeper knowledge of customized treatment options for BRCA. In order to quickly discover and optimize medication combinations for targeted pyroptosis treatment in TNBC, our group created the AI model biological factor-regulated neural network (BFReg-NN) (Fig. 11B) [172]. Large TNBC patient and drug databases are analyzed by the model, which combines bioinformatics, AI, and experimental validation. Based on the genes linked to pyroptosis, the model predicts compound medications that may cause TNBC pyroptosis. Four layers make up the BFReg-NN model: the survival layer, the drug-target relationship layer, the drug-target to pyroptosis gene connecting layer, and the pyroptosis s gene relationship layer. A thorough grasp of the mechanisms involved can be obtained by employing a graph neural network to learn how intracellular biological components (such as genes, proteins, or medication targets) interact with one another and how these factors operate inside the cell. Interestingly, twelve selected drug pairs all could synergistically induce

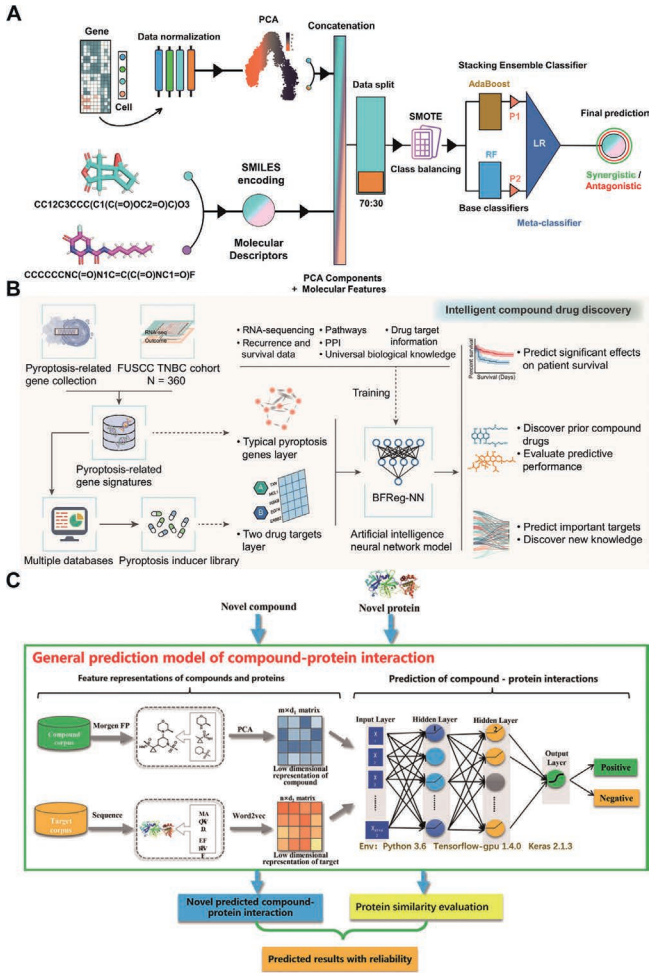


Fig. 11. AI models applied to the discovery of compound medicines. (A) The workflow for DDSBC learning architecture. Reproduced with permission [171]. Copyright 2024, American Chemical Society. (B) The workflow for discovering and optimizing anti-TNBC compound pyroptosis drugs based on big data and AI. Reproduced with permission [172]. Copyright 2024, Springer Nature. (C) The architecture of the CPI prediction model. Reproduced with permission [173]. Copyright 2024, The Authors.

TNBC pyroptosis, suggesting a high prediction accuracy of synergistic drug pairs. Generally, this model has significant implications for discovering drug pairs for precision treatment of refractory diseases. Ji *et al.* used a global compound-protein-interactions (CPI) prediction model based on DL to find possible chemical medications used in traditional Chinese medicine (TCM) (Fig. 11C) [173]. Using *Hedyotis Diffusa* and *Astragalus* as examples, they were able to identify synergistic anti-tumor multi-compound combinations and correctly anticipate the therapeutic targets of the active chemicals in these herbs. According to experimental data, the MDA-MB-231 BRCA cell line demonstrated notable anti-tumor effects from the projected multi-compound combinations. Combination I, for example, showed synergy with an IC_{50} of 19.41 μmol/L and a CI value of 0.682. This combination comprises epicatechin, ursolic acid, quercetin, 7-epioxysterol, and astragaloside IV.

Collectively, these AI-driven approaches demonstrate vital potential for clinical translation. Experimentally validated models (*e.g.*, RiboStrike, Gex2SGen) show immediate applicability due to their biological verification, while multi-modal integrated systems (*e.g.*, MOMLIN, FAIS-DL) align closely with clinical workflows. Drug repurposing frameworks (GraphRepur, ResisenseNet) offer near-term clinical value through redeployment of existing therapeutics. Future efforts should prioritize multi-center validation to advance these models toward clinical implementation.

5. Challenges and remedies in the application of AI in BRCA

AI, particularly ML and DL, has emerged as a crucial diagnostic, therapeutic, and prognostic tool for BRCA, providing notable benefits in terms of accuracy and efficiency. It offers new theoretical frameworks and practical viewpoints for dealing with the complexity of BRCA, which is typified by a variety of pathogenic kinds, complicated genetic subtypes, tumor heterogeneity, and the fact that it is frequently undetectable, making early identification difficult. Notwithstanding these developments, there are still a number of obstacles to overcome before AI models may be used in clinical settings. These obstacles include problems with data quality, model performance, interpretability, clinical validation, and ethical compliance. Table 1 offers a comprehensive overview of the challenges encountered by AI models in the field of BRCA, along with the solutions proposed to address them.

5.1. Challenges in data quality

The caliber of data is a critical determinant constraining the efficacy of AI models. First of all, issues like single-center bias (as shown in the RSF-RFE model, which fails to take ethnic diversity into account [25]) and limited sample sizes (the CE-CBBCT research, for example, only comprised 56 patients [19]) seriously impair models' capacity to generalize. Further decreasing the applicability of radiomics models is feature drift, which can be caused by imaging discrepancies between devices (*e.g.*, variations in ultrasound settings or MRI protocols) [177,178]. Creating high-quality datasets is also significantly hampered by several other problems, such as the lack of dynamic data (genomic or metabolomic changes during treatment), the need for expert judgment in data labeling (especially because of labeling errors resulting from ambiguous pathological boundaries in BRCA), and the high expense of labeling [179]. One possible way to address these issues is by using dynamic data systems. High-quality data serves as the foundation for AI models' ongoing development. It is possible to create cooperative worldwide multicenter networks to share standardized data across devices and geographies. For example, the RadioVal project combined five TCIA BRCA datasets, totaling 2035 patients, and used the FAIR principles to guarantee data interoperability [178]. Additionally, uncommon subtype data (such as TNBC) may be supplemented with high-quality pathological pictures produced by GANs, and the model's capacity for generalization can be improved by utilizing transfer learning approaches [180]. Automated tools, such as RV-Cherry-Picker, can be developed to extract key features from DICOM metadata. By combining dynamic modeling techniques, like LSTM networks, with ctDNA mutation trajectories and DCE-MRI imaging data, real-time tracking of chemotherapy resistance evolution can be achieved [181]. The technologies employed in the aforementioned research play a key role in building dynamic data systems, driving the achievement of high-quality and standardized data. Moving forward, the focus should remain on multimodal integration, active learning, and distributed collaboration, transitioning AI from being dependent on data quantity to leveraging data intelligence, which will establish a strong foundation for the advancement of AI in precision medicine.

5.2. Model efficacy and generalization difficulties

Both performance and generalization are major problems for current approaches. Radiomics models have trouble extracting cross-modal features, including connecting MRI pictures with pathologic slice data, and are extremely susceptible to device noise. The deployment of DL models in primary care settings is further limited since they require specialist equipment (*e.g.*, BSGI requires radioactive isotopes [74]) and high-performance hardware (*e.g.*,

Table 1
Challenges and proposed solutions for AI models in BRCA applications.

Category	Key challenge	Solution/technology	Exemplar case/tool
Data quality	Single-center bias, limited sample sizes, feature drift induced by cross-device heterogeneity	Multicenter collaborative networks, synthetic data generation *via* GANs, federated learning	RadioVal project (FAIR-compliant data integration), RV-Cherry-Picker (DICOM metadata extraction)
Model performance	Cross-modal feature extraction limitations, hardware dependency (*e.g.*, GPU clusters)	Hybrid architectures (Transformer-GNN integration), lightweight model distillation	ResisenseNet (cross-cancer adaptation), RF-Fastify (edge computing optimization)
Dynamic adaptation	Static prediction frameworks failing to capture therapeutic dynamics	LSTM-based temporal modeling, ctDNA-MRI multimodal fusion for real-time surveillance	3D-GCN (radiotherapy simulation), BITES (immune-metabolic causal inference)
Interpretability	Opaque decision mechanisms, insufficient RCT validation	SHAP/Grad-CAM visualization techniques, three-phase validation cycle (AI screening $\rightarrow$*in vitro* validation $\rightarrow$ clinical feedback)	STITCH pathway reconstruction (protein interaction mapping)
Multimodal fusion	Disjointed imaging-omics-clinical data integration	Imaging genomics frameworks, dynamic meta-learning architectures	Transformer-enhanced radiogenomic cross-analysis models
Ethical compliance	Data privacy risks, accountability ambiguity, resource allocation disparities	Adaptive federated learning contracts, cost-effective edge computing deployment	OMOP-CDM standardized databases, DICOM-MIABIS cross-institutional protocols
Technological development directions	Absence of full-cycle AI toolkits, inadequate biological mechanism exploration	Free energy perturbation (FEP)-guided drug simulation, 3D dynamic molecular modeling	Intraoperative AI-pathology integration platforms

A100 GPU clusters) [182–185]. Furthermore, only a small number of models can integrate imaging, omics, and clinical time-series data, and multimodal data fusion technologies are still in their infancy [186–188]. Solutions balancing clinical applicability and performance optimization are being investigated to overcome these problems. As an example, hybrid architectures that combine Transformer and GNN are being utilized to improve cross-modal feature extraction by dynamically analyzing the spatial correlations between radiomics characteristics and single-cell data from tumor microenvironments. For low-latency applications like intraoperative ultrasound navigation, knowledge distillation techniques like MobileNet/ShuffleNet are being used to reduce model size [189,190]. Moreover, lightweight tools like RF-Fastify are being developed to reduce deployment obstacles in basic healthcare facilities [191,192], and meta-learning frameworks like ResisenseNet are enabling the cross-domain transfer of models to related malignancies, such as ovarian cancer [193].

5.3. Interpretability and validation system difficulties

There are now questions regarding trust in therapeutic applications due to the "black box" nature of AI models. Despite relying on implicit feature correlations, DL algorithms have not been physiologically verified through immunological microenvironments or biochemical pathways, raising questions about the validity of decision-making processes. With just 57 % of AI tools completely created and 67 % missing sufficient validation, there is also a dearth of thorough RCT validation for radiomics investigations [194]. The lack of experimental input from PDX or organoid models worsens the situation for drug prediction models, such as those employed for target screening. Furthermore, it is difficult to measure the additional clinical value of AI systems due to the paucity of traditional risk-benefit comparison studies of diagnostic and treatment approaches [194]. Enhancing clinical interpretability is one way to remedy this. Visual tools such as SHAP and Grad-CAM, for instance, can assist in identifying important areas for decision-making (such as the biological relationship between HER2 receptor epitopes and molybdenum target calcification) [195,196], and the STITCH protein interaction database can be used to create mechanism-driven knowledge graphs [197,198]. Another strategy is to create a three-phase cycle system of "AI screening, *in vitro* validation, clinical feedback," validate drug combinations using PDX and PDO models, and conduct multi-center prospective RCTs to evaluate improvements in survival outcomes and the FNR of AI tools [199].

5.4. Standardization and ethical difficulties

Ethical quandaries and the lack of well-defined technological standards limit the ethical application of AI in healthcare. In high-stakes oncological decision-making, specific clinical risks stemming from AI model hallucinations, bias, and dataset heterogeneity pose substantial threats to patient safety and treatment equity. Model hallucinations, where complex algorithms generate plausible yet inaccurate predictions (*e.g.*, misclassification of HER2-low subtypes or overestimation of chemotherapy response), may lead to inappropriate therapeutic adjustments, such as unnecessary invasive interventions or delayed initiation of targeted therapy, directly compromising patient outcomes. This risk is exacerbated by the "black box" nature of advanced models, where erroneous outputs are challenging to identify in clinical practice [200]. Dataset bias further amplifies disparities: single-center training datasets often underrepresent rare subtypes (*e.g.*, TNBC) or specific demographic groups, resulting in degraded performance in diverse clinical settings, analogous to the limitations observed in single-center studies on perioperative neurocognitive disorder prediction [201]. Additionally, cross-institutional heterogeneity in imaging protocols (*e.g.*, MRI acquisition parameters) or pathological annotation criteria introduces feature drift, reducing model reliability when deployed across multiple centers and potentially widening healthcare disparities [200,201].

Regulations govern the privacy of medical data, and although federated learning helps prevent direct data sharing, data gathering robustness still has to be improved [202]. There is still disagreement about who should bear the blame for AI misdiagnoses: the operator, the hospital, or the developer [203,204]. The disparity in resources between primary care and big medical facilities is further exacerbated by the dependence on costly technologies and high operating expenses [205]. Furthermore, inadequate AI training for medical professionals might result in forecasts being misinterpreted. To tackle these issues, we suggest creating a federated learning architecture that complies with privacy regulations and putting in place flexible contracts to define accountability [206,207]. Cost-effective models for primary hospitals should be developed, such as intraoperative decision-support systems modified for edge computing. It is also necessary to build training tools

(such as platforms that integrate AI with intraoperative frozen pathology) to enhance the critical thinking skills of healthcare personnel. Transparency in data updating processes may also be ensured by supporting standardized data types like DICOM-MIABIS and OMOP-CDM and creating tools like RV-Cherry-Picker that can dynamically adapt to molecular subtyping evolution [178].

5.5. Challenges in technological iteration and evolving diagnostic and treatment paradigms

There is currently no complete, full-cycle toolchain that covers screening, diagnosis, therapy, and follow-up, and AI research is still restricted to static forecasts. A better knowledge of biological mechanisms is hindered by the old "black box" output paradigm, and diagnostic and treatment systems also suffer with dynamic responsiveness (for instance, the inability to adapt in real-time depending on changes in adjuvant chemotherapy regimens). Static forecasts must give way to dynamic, responsive tracking in order to overcome these difficulties. This would include, for example, developing a ctDNA-MRI fusion model that functions as an adjuvant therapy early warning system, allowing for dynamic therapeutic grading and real-time treatment modifications. Building a comprehensive AI-assisted platform that covers the full treatment cycle may also be facilitated by using imaging genomics technologies. Drug-target binding effectiveness and radiotherapy distribution may be predicted by combining free energy perturbation simulations with three-dimensional dynamic models, such as 3D-GCN [208]. Additionally, by breaking the closed loop for biological mechanism analysis, the use of causal inference models (such as BITES) may aid in quantifying the connection between immune evasion and lipid metabolism reprogramming.

6. Conclusion and perspectives

The swift development of AI is revolutionizing the detection and treatment of BRCA and giving precision medicine a new lease of life. This review thoroughly explores the innovative uses of AI in clinical decision-making and drug development for BRCA, emphasizing the technology's key benefits in determining molecular subtypes, predicting tumor status, estimating the risk of metastasis or recurrence, and refining treatment plans. Notably, beyond HER2-low subtypes, AI demonstrates significant promise in addressing the clinical challenges of TNBC. For instance, AI-driven analysis of multiparametric MRI achieves AUCs up to 0.86 for TNBC subtype classification [209], while serum Raman spectroscopy combined with CNN models attains 91.11 % accuracy in non-invasive detection [210]. Surface-enhanced Raman scattering (SERS) platforms further enable label-free cancer screening with 95 % accuracy [211]. In therapy, AI-guided drug delivery systems (*e.g.*, disulfide bond-engineered nanoassemblies suppressing tumors by $>$70 % with reduced toxicity [212]) and metabolic vulnerability identification (*e.g.*, targeting glutamine dependency in Lehmann subtypes [213]) exemplify transformative TNBC applications.

AI expands the potential for individualized therapy while also overcoming the drawbacks of traditional approaches by fusing multimodal data with state-of-the-art algorithms. Crucially, AI extends to immunotherapy response prediction through inflammatory indices like baseline systemic immune-inflammation index (SII), which independently prognosticates survival outcomes in HER2-positive metastatic disease [214], and deciphers metabolic reprogramming (*e.g.*, IDO-mediated tryptophan metabolism) linked to immune evasion in TNBC[213].

The present state of research still faces a number of obstacles, such as heterogeneous data, inconsistent annotations, poor interpretability of the models, a lack of strong clinical translation validation, and intricate ethical and privacy issues. The development of more robust cross-center and cross-device models, utilizing methods such as federated learning to improve data utilization, the advancement of the integration of multi-omics data with imaging and pathological features to create a dynamic digital twin of the tumor, the promotion of the use of explainable AI in conjunction with causal reasoning to identify the biomarker networks influencing clinical outcomes, and the construction of a real-time feedback system for AI-assisted decision-making, allowing for ongoing optimization of diagnosis and treatment, should be the main areas of future research. Accelerating AI-driven target identification and medication repositioning is crucial in the drug development industry. Virtual clinical trial frameworks should also be investigated. Notably, the development of large language models in biomedical research has the potential to transform AI into a potent link between fundamental research and clinical practice, allowing the switch from "data-driven" to "knowledge-driven" methods in the treatment of BRCA.

In summary, a new "intelligent oncology" paradigm will develop as a result of the extensive integration of AI into BRCA treatment. It is projected that a fully integrated, intelligent system encompassing early screening, diagnosis, treatment, and prognosis management will soon be realized with continued technological advancements and interdisciplinary collaboration, leading to more effective, accurate, and reasonably priced care for patients.

CRediT authorship contribution statement

Ting Wang: Writing – review & editing, Writing – original draft, Validation, Supervision, Formal analysis, Data curation, Conceptualization. **Xifeng Qin:** Writing – review & editing, Validation, Supervision, Conceptualization. **Yao Liu:** Supervision. **Jianhui Tian:** Validation, Supervision. **Zhiqing Pang:** Writing – review & editing, Validation, Supervision, Conceptualization.

Declaration of competing interest

The authors declare that they have no known competing financial interests or personal relationships that could have appeared to influence the work reported in this paper.

Acknowledgment

This work was supported by the National Key Research and Development Program of China (No. 2024YFA0919100).

Supplementary materials

Supplementary material associated with this article can be found, in the online version, at doi:10.1016/j.cclet.2025.111956.

References

[1] C. Zhang, J. Xu, R. Tang, et al., J. Hematol. Oncol. 16 (2023) 114.
[2] R. Gupta, D. Srivastava, M. Sahu, et al., Mol. Divers. 25 (2021) 1315–1360.
[3] R.Y. Choi, A.S. Coyner, J. Kalpathy-Cramer, et al., Transl. Vis. Sci. Technol. 9 (2020) 14.
[4] S. Yan, J. Li, W. Wu, J. Cancer Res. Clin. Oncol. 149 (2023) 16179–16190.
[5] J. Guo, J. Hu, Y. Zheng, et al., Br. J. Cancer 128 (2023) 2141–2149.
[6] C. Zhang, L. Zhang, D. Yang, et al., Chin. Chem. Lett. (2025), doi:10.1016/j.cclet.2025.111828.
[7] H. Sung, J. Ferlay, R.L. Siegel, et al., CA Cancer J. Clin. 71 (2021) 209–249.
[8] Y. Gao, S. Ventura-Diaz, X. Wang, et al., Nat. Commun. 15 (2024) 9613.
[9] R.L. Siegel, K.D. Miller, N.S. Wagle, A. Jemal, CA Cancer J. Clin. 73 (2023) 17–48.
[10] B.S. Chhikara, K. Parang, Chem. Biol. Lett. 10 (2023) 451.
[11] T. Li, Y. Zhang, S. Che, et al., Chin. Chem. Lett. 37 (2026) 111936.
[12] E. Nolan, G.J. Lindeman, J.E. Visvader, Cell 186 (2023) 1708–1728.
[13] E.N. Bergstrom, A. Abbasi, M. Diaz-Gay, et al., J. Clin. Oncol. 42 (2024) 3550–3560.
[14] Z. Xiong, K. Liu, S. Liu, et al., BMC Cancer 24 (2024) 1204.
[15] C. Boissin, Y. Wang, A. Sharma, et al., Breast Cancer Res. 26 (2024) 90.

[16] S. Alaeikhanehshir, M.M. Voets, F.H. van Duijnhoven, et al., Cancer Imaging 24 (2024) 48.
[17] S. Krishnamurthy, S.J. Schnitt, A. Vincent-Salomon, et al., JCO Precis. Oncol. 8 (2024) e2400353.
[18] Y. Guo, X. Xie, W. Tang, et al., Eur. Radiol. 34 (2024) 899–913.
[19] X. Chen, M. Li, X. Liang, D. Su, Medicine 103 (2024) e38513.
[20] F. Marme, E. Krieghoff-Henning, B. Gerber, et al., Eur. J. Cancer 195 (2023) 113390.
[21] T. Zhu, Y.H. Huang, W. Li, et al., Int. J. Surg. 109 (2023) 3383–3394.
[22] Y. Yu, R. Chen, J. Yi, et al., Breast 77 (2024) 103786.
[23] R. Cai, L. Deng, H. Zhang, H. Zhang, Q. Wu, Radiat. Oncol. 19 (2024) 63.
[24] R. Shahriarirad, S.M. Meshkati Yazd, R. Fathian, et al., Sci. Rep. 14 (2024) 1351.
[25] H. Li, R.B. Liu, C.M. Long, et al., Cancer Rep. 7 (2024) e2006.
[26] Y. Yu, W. Ren, Z. He, et al., Breast Cancer Res. 25 (2023) 132.
[27] J. Han, H. Hua, J. Fei, et al., Clin. Breast Cancer 24 (2024) 215–226.
[28] Z. Xu, Y. Xie, L. Wu, et al., J. Magn. Reson. Imaging 58 (2023) 1580–1589.
[29] A.C. Wolff, M.E.H. Hammond, K.H. Allison, et al., J. Clin. Oncol. 36 (2018) 2105–2122.
[30] L. Liu, Z. Zhao, F. Zou, et al., Chin. Chem. Lett. 36 (2025) 111451.
[31] S. Modi, W. Jacot, T. Yamashita, et al., N. Engl. J. Med. 387 (2022) 9–20.
[32] M. Wesoła, M. Jeleń, Adv. Clin. Exp. Med. 24 (2015) 899–903.
[33] H.C. Hwang, A.M. Gown, Methods Mol. Biol. 1406 (2016) 61–70.
[34] M. Liu, L. Xi, T. Tan, et al., Chin. Chem. Lett. 32 (2021) 1726–1730.
[35] Y. Zhu, A.M. O'Connell, Y. Ma, et al., Eur. Radiol. 32 (2022) 2286–2300.
[36] M.D. Ryser, D.L. Weaver, F. Zhao, et al., J. Natl. Cancer Inst. 111 (2019) 952–960.
[37] O. Ronneberger, P. Fischer, T. Brox, U-Net: convolutional networks for biomedical image segmentation, in: N. Navab, J. Hornegger, W. Wells, A.A. Frangi (Eds.), Proceedings of the MICCAI, Cham, Springer, 2015, pp. 234–241.
[38] R.L. Schilsky, D.L. Longo, N. Engl. J. Med. 387 (2022) 2107–2110.
[39] R. Prakash, Y. Zhang, W. Feng, M. Jasin, Cold Spring Harb. Perspect. Biol. 7 (2015) a016600.
[40] P.A. Ascierto, C. Bifulco, G. Palmieri, S. Peters, N. Sidiropoulos, J. Mol. Diagn. 21 (2019) 756–767.
[41] C.W. Elston, I.O. Ellis, Histopathology 19 (1991) 403–410.
[42] H.J. Bloom, W.W. Richardson, Br. J. Cancer 11 (1957) 359–377.
[43] E.A. Rakha, J.S. Reis-Filho, F. Baehner, et al., Breast Cancer Res. 12 (2010) 207.
[44] B. Acs, I. Fredriksson, C. Rönnlund, et al., Cancers 13 (2021) 1166.
[45] C. van Dooijeweert, P.J. van Diest, S.M. Willems, et al., Int. J. Cancer 146 (2020) 769–780.
[46] V. Lorgis, M.P. Algros, C. Villanueva, et al., Breast 20 (2011) 284–287.
[47] Y. Wang, B. Acs, S. Robertson, et al., Ann. Oncol. 33 (2022) 89–98.
[48] B. Medeiros, A.L. Allan, Int. J. Mol. Sci. 20 (2019) 2272.
[49] Y.Z. Zheng, X.M. Wang, L. Fan, Z.M. Shao, Oncologist 26 (2021) e241–e250.
[50] W. Voon, Y.C. Hum, Y.K. Tee, et al., Sci. Rep. 13 (2023) 20518.
[51] A. Adam Maciejczyk, Adv. Clin. Exp. Med. 22 (2013) 5–15.
[52] F. Cardoso, L.J. van't Veer, J. Bogaerts, et al., N. Engl. J. Med. 375 (2016) 717–729.
[53] H. Ishwaran, U.B. Kogalur, X. Chen, A.J. Minn, Stat. Anal. Data Min. ASA Data Sci. J. 4 (2011) 115–132.
[54] L. Breiman, Mach. Learn. 45 (2001) 5–32.
[55] K. Moorthy, M.S. Mohamad, Bioinformation 7 (2011) 142–146.
[56] M. Ram, A. Najafi, M.T. Shakeri, Iran. J. Pathol. 12 (2017) 339–347.
[57] H.S. Cody, Breast Cancer 6 (1999) 13–22.
[58] D. Krag, D. Weaver, T. Ashikaga, et al., N. Engl. J. Med. 339 (1998) 941–946.
[59] J.M. Johnson, R.K. Orr, S.R. Moline, Am. Surg. 67 (2001) 1030–1033.
[60] E.E. Sanidas, E. de Bree, D.D. Tsiftsis, Am. J. Surg. 185 (2003) 202–210.
[61] T. Kuehn, I. Bauerfeind, T. Fehm, et al., Lancet Oncol. 14 (2013) 609–618.
[62] J.C. Boughey, V.J. Suman, E.A. Mittendorf, et al., JAMA 310 (2013) 1455–1461.
[63] S.M. Bentzen, R.K. Agrawal, E.G. Aird, et al., Lancet Oncol. 9 (2008) 331–341.
[64] S.Ö. Arik, T. Pfister, in: Proceedings of the AAAI Conference on Artificial Intelligence, 35, 2021, pp. 6679–6687.
[65] E.W.S. Soares, H.M. Nagai, L.C. Bredt, et al., World J. Surg. Oncol. 12 (2014) 67.
[66] K. Dinas, M. Kalder, L. Zepiridis, et al., Curr. Probl. Cancer 43 (2019) 100470.
[67] A. Husted Madsen, K. Haugaard, J. Soerensen, et al., Breast 17 (2008) 138–147.
[68] P. Del Bianco, G. Zavagno, P. Burelli, et al., Eur. J. Surg. Oncol. 34 (2008) 508–513.
[69] A.I. Huppe, A.K. Mehta, R.F. Brem, Semin. Ultrasound CT MRI 39 (2018) 60–69.
[70] T.M. Kolb, J. Lichy, J.H. Newhouse, Radiology 225 (2002) 165–175.
[71] D. Yue, M. Wang, F. Deng, et al., Chin. Chem. Lett. 29 (2018) 648–656.
[72] D.J. Rhodes, C.B. Hruska, A.L. Conners, et al., AJR Am. J. Roentgenol. 204 (2015) 241–251.
[73] L.R. Rechtman, M.J. Lenihan, J.H. Lieberman, et al., AJR Am. J. Roentgenol. 202 (2014) 293–298.
[74] J. Villanueva-Meyer, M.H. Leonard Jr., E. Briscoe, et al., J. Nucl. Med. 37 (1996) 926–930.
[75] J. Werner, J.A. Rapelyea, K.G. Yost, R.F. Brem, Breast J. 15 (2009) 579–582.
[76] B.T. Hennessy, G.N. Hortobagyi, R. Rouzier, et al., J. Clin. Oncol. 23 (2005) 9304–9311.
[77] B.T. Hennessy, A.M. Gonzalez-Angulo, G.N. Hortobagyi, et al., Cancer 106 (2006) 1000–1006.
[78] W.J. Gradishar, M.S. Moran, J. Abraham, et al., J. Natl. Compr. Cancer Netw. 20 (2022) 691–722.
[79] J. Li, J. Zhou, H. Wang, et al., JAMA Netw. Open 6 (2023) e2321388.
[80] L.M. Spring, Y. Bar, S.J. Isakoff, J. Natl. Compr. Cancer Netw. 20 (2022) 723–734.
[81] E.J. Diego, P.F. McAuliffe, A. Soran, et al., Ann. Surg. Oncol. 23 (2016) 1549–1553.
[82] L.S. Dominici, V.M. Negron Gonzalez, A.U. Buzdar, et al., Cancer 116 (2010) 2884–2889.
[83] J.C. Boughey, L.M. McCall, K.V. Ballman, et al., Ann. Surg. 260 (2014) 608–614.
[84] M. Colleoni, Z. Sun, K.N. Price, et al., J. Clin. Oncol. 34 (2016) 927–935.
[85] A. Sparano Joseph, J. Gray Robert, F. Makower Della, et al., N. Engl. J. Med. 373 (2015) 2005–2014.
[86] W.J. Gradishar, B.O. Anderson, J. Abraham, et al., J. Natl. Compr. Cancer Netw. 18 (2020) 452–478.
[87] E.A. Rakha, A. Abbas, P. Pinto Ahumada, et al., J. Clin. Pathol. 71 (2018) 802.
[88] E.A. Rakha, S. Martin, A.H.S. Lee, et al., Cancer 118 (2012) 3670–3680.
[89] G. Houvenaeghel, M. Cohen, J.M. Classe, et al., ESMO Open 6 (2021) 100316.
[90] Y.M. Zhong, F. Tong, J. Shen, BMC Cancer 22 (2022) 102.
[91] A.S. Hamy, G.T. Lam, E. Laas, et al., Breast Cancer Res. Treat. 169 (2018) 295–304.
[92] Z. Huang, Q. Peng, L. Mao, et al., MedComm Future Med 4 (2025) e70013.
[93] X. Li, C. Li, H. Wang, L. Jiang, M. Chen, PeerJ 12 (2024) e17683.
[94] Y. Lin, J. Wang, M. Li, et al., Breast 76 (2024) 103737.
[95] G. Zheng, J. Peng, Z. Shu, et al., J. Cancer Res. Clin. Oncol. 150 (2024) 147.
[96] Z. Li, J. Gao, H. Zhou, et al., EBioMedicine 107 (2024) 105311.
[97] A. Fanizzi, A. Latorre, D.A. Bavaro, et al., Cancer Med. 12 (2023) 20663–20669.
[98] O. Falou, L. Sannachi, M. Haque, et al., Sci. Rep. 14 (2024) 2340.
[99] J. Gu, X. Zhong, C. Fang, et al., Oncologist 29 (2024) e187–e197.
[100] X. Zheng, Z. Yao, Y. Huang, et al., Nat. Commun. 11 (2020) 1236.
[101] Y. Xie, J. Zhang, Y. Xia, et al., Inf. Fusion 42 (2018) 102–110.
[102] D. Fornvik, S. Borgquist, M. Larsson, et al., Eur. J. Radiol. 178 (2024) 111624.
[103] S. Chen, K. Ma, Y. Zheng, ArXiv (2019), doi:10.48550/arXiv.1904.00625.
[104] R.R. Selvaraju, M. Cogswell, A. Das, et al., Grad-CAM: visual explanations from deep networks *via* gradient-based localization, in: Proceedings of the IEEE International Conference on Computer Vision, 2017, pp. 618–626.
[105] J. Adebayo, J. Gilmer, M. Muelly, et al., Sanity checks for saliency maps, in: Proceedings of the 32nd Conference on Neural Information Processing Systems (NeurIPS 2018), 2018, pp. 9525–9536.
[106] D. Xing, Y. Lv, B. Sun, et al., Acad. Radiol. 31 (2024) 3524–3534.
[107] K. Saednia, W.T. Tran, A. Sadeghi-Naini, Med. Phys. 50 (2023) 7852–7864.
[108] W. Aswolinskiy, E. Munari, H.M. Horlings, et al., Breast Cancer Res. 25 (2023) 142.
[109] M. Yoneyama, K. Zormpas-Petridis, R. Robinson, et al., Int. J. Radiat. Oncol. Biol. Phys. 120 (2024) 862–874.
[110] E. Zhu, L. Zhang, Y. Liu, et al., Clin. Transl. Oncol. 26 (2024) 2584–2593.
[111] S. Schrod, A. Schäfer, S. Solbrig, et al., Bioinformatics 38 (2022) i60–i67.
[112] S.R. Künzel, J.S. Sekhon, P.J. Bickel, B. Yu, Proc. Natl. Acad. Sci. USA 116 (2019) 4156–4165.
[113] S. Benzekry, M. Mastri, C. Nicolo, J.M.L. Ebos, PLoS Comput. Biol. 20 (2024) e1012088.
[114] X. Han, Y. Guo, H. Ye, et al., Breast Cancer Res. 26 (2024) 18.
[115] E. Zhu, L. Zhang, J. Wang, et al., Breast Cancer Res. Treat. 205 (2024) 97–107.
[116] K. Dell'Aquila, A. Vadlamani, T. Maldjian, et al., Breast Cancer Res. 26 (2024) 7.
[117] Y. Tong, Z. Hu, H. Wang, et al., Eur. Radiol. 34 (2024) 5477–5486.
[118] H. Zhu, H. Hu, B. Hao, et al., Technol. Cancer Res. Treat. 23 (2024) 15330338241263434.
[119] M.E. Ritchie, B. Phipson, D. Wu, et al., Nucleic Acids Res. 43 (2015) e47.
[120] P. Langfelder, S. Horvath, BMC Bioinform. 9 (2008) 559.
[121] J. Friedman, T. Hastie, R. Tibshirani, J. Stat. Softw. 33 (2010) 1–22.
[122] R. Marshall. regplot: enhanced regression nomogram plot (Version 1.1) [Computer software] 2020. 10.32614/CRAN.package.regplot.
[123] H. Ma, L. Shi, J. Zheng, et al., BMC Cancer 24 (2024) 1222.
[124] B. Wu, L. Li, L. Li, et al., Genes 15 (2024) 1093.
[125] M. Piffoux, J. Jacquemin, M. Petera, et al., Clin. Cancer Res. 30 (2024) 4654–4666.
[126] J.A. Pogue, J. Harms, C.E. Cardenas, et al., Phys. Med. Biol. 69 (2024), doi:10.1088/1361-6560/ad4a1c.
[127] U. Schulz, M. Busch, U. Bormann, Int. J. Radiat. Oncol. Biol. Phys. 10 (1984) 915–920.
[128] M.J. Rivard, B.M. Coursey, L.A. DeWerd, et al., Med. Phys. 31 (2004) 633–674.
[129] C.M. Ma, J.S. Li, S.B. Jiang, et al., Phys. Med. Biol. 50 (2005) 891.
[130] S. Quetin, B. Bahoric, F. Maleki, S.A. Enger, Phys. Med. Biol. 69 (2024), doi:10.1088/1361-6560/ad3dbd.
[131] L.C. Moore, F. Nematollahi, L. Li, et al., Med. Phys. 51 (2024) 7453–7463.
[132] T. Tsui, A. Podgorsak, J.C. Roeske, et al., J. Appl. Clin. Med. Phys. 25 (2024) e14461.
[133] C. Boutry, N.N. Moreau, C. Jaudet, et al., Radiother. Oncol. 200 (2024) 110483.
[134] S. Cui, G. Li, H.C. Kuo, et al., J. Appl. Clin. Med. Phys. 25 (2024) e14216.
[135] S. Zhang, B. Yang, H. Yang, et al., Sci. Bull. 69 (2024) 1748–1756.
[136] A. Maniscalco, E. Mathew, D. Parsons, et al., Med. Phys. 51 (2024) 3932–3949.
[137] Y. Mao, W. Di, D. Zong, et al., J. Appl. Clin. Med. Phys. 25 (2024) e14194.
[138] M. Lepomäki, U. Karhunen-Enckell, J. Tuominen, et al., J. Surg. Oncol. 125 (2022) 577–588.
[139] C. Yeung, T. Ungi, Z. Hu, et al., Int. J. Comput. Assist. Radiol. Surg. 19 (2024) 1193–1201.
[140] C. Apelian, F. Harms, O. Thouvenin, A.C. Boccara, Biomed. Opt. Express 7 (2016) 1511–1524.

[141] B. Dolega-Kozierowski, P. Kasprzak, M. Lis, et al., Breast Cancer Res. Treat. 202 (2023) 33–43.
[142] G. Liang, W. Fan, H. Luo, X. Zhu, Biomed. Pharmacother. 128 (2020) 110255.
[143] M. Sufyan, Z. Shokat, U.A. Ashfaq, Comput. Biol. Med. 165 (2023) 107356.
[144] Q. Zhang, D. Chen, Drug Dev. Res. 85 (2024) e22223.
[145] J. Alexander, K. Schipper, S. Nash, et al., Br. J. Cancer 130 (2024) 1828–1840.
[146] X. Chen, J. Yi, L. Xie, et al., Front. Immunol. 15 (2024) 1470167.
[147] M.M. Rashid, K. Selvarajoo, Brief. Bioinform. 25 (2024) bbae300.
[148] S. Pawar, T.O. Liew, A. Stanam, C. Lahiri, Chem. Biol. Drug Des. 96 (2020) 995–1004.
[149] A.C. Kaushik, Z. Zhao, Front. Mol. Biosci. 10 (2023) 1215204.
[150] M. Kováčová, V. Hlavac, R. Kozevnikovova, et al., Oncology 102 (2024) 1029–1040.
[151] J. Fucikova, O. Kepp, L. Kasikova, et al., Cell Death Dis. 11 (2020) 1013.
[152] A. Ahmed, S.W.G. Tait, Mol. Oncol. 14 (2020) 2994–3006.
[153] K. Hayashi, F. Nikolos, Y.C. Lee, et al., Nat. Commun. 11 (2020) 6299.
[154] H. Deng, W. Yang, Z. Zhou, et al., Nat. Commun. 11 (2020) 4951.
[155] H. Ruan, B.J. Leibowitz, L. Zhang, J. Yu, Mol. Carcinog. 59 (2020) 783–793.
[156] P. Li, W. Wang, S. Wang, et al., Front. Immunol. 14 (2023) 1145481.
[157] D. Yang, L. Wang, P. Yuan, et al., Chin. Chem. Lett. 34 (2023) 107964.
[158] A. Keshavarzi Arshadi, M. Salem, H. Karner, et al., Patterns 5 (2024) 100909.
[159] D. Das, B. Chakrabarty, R. Srinivasan, A. Roy, J. Chem. Inf. Model. 63 (2023) 1882–1893.
[160] T. Wen, J. Wang, R. Lu, et al., Eur. J. Med. Chem. 250 (2023) 115199.
[161] A. Karampuri, S. Kundur, S. Perugu, Comput. Biol. Med. 174 (2024) 108433.
[162] Y. Gao, S. Chen, J. Tong, X. Fu, BMC Bioinform. 23 (2022) 382.
[163] C. Cui, X. Ding, D. Wang, et al., Bioinformatics 37 (2021) 2930–2937.
[164] A. Karampuri, B.K. Jakkula, S. Perugu, Sci. Rep. 14 (2024) 23949.
[165] Z.Y. Li, Y.X. Zhu, J.R. Chen, et al., Biomed. Pharmacother. 162 (2023) 114661.
[166] S. Zhao, T. Nishimura, Y. Chen, et al., Sci. Transl. Med. 5 (2013) 206ra140.
[167] P. Csermely, T. Korcsmáros, H.J.M. Kiss, et al., Pharmacol. Ther. 138 (2013) 333–408.
[168] J.A. Hill, R. Ammar, D. Torti, et al., PLos Genet. 9 (2013) e1003390.
[169] A.D. Verderosa, R. Dhouib, Y. Hong, et al., Sci. Rep. 11 (2021) 1569.
[170] P. Li, C. Huang, Y. Fu, et al., Bioinformatics 31 (2015) 2007–2016.
[171] A. Mehmood, A.C. Kaushik, D.Q. Wei, J. Chem. Inf. Model. 64 (2024) 6421–6431.
[172] B. Ouyang, C. Shan, S. Shen, et al., Nat. Commun. 15 (2024) 7560.
[173] W. Ji, S. She, C. Qiao, et al., Front. Pharmacol. 15 (2024) 1465890.
[174] Y. Chen, B. Li, X. Chen, et al., Chin. Chem. Lett. 31 (2020) 1153–1158.
[175] J. Zhu, Y. Xiong, X. Bai, et al., Chin. Chem. Lett. 36 (2025) 110799.
[176] A. Mehmood, M.S. Ali, D. Li, et al., Chem. Biol. Drug Des. 104 (2024) e14627.
[177] X. Wu, W. Li, H. Tu, Trends Cancer 10 (2024) 147–160.
[178] V. Kilintzis, V. Kalokyri, H. Kondylakis, et al., Eur. Radiol. Exp. 8 (2024) 42.
[179] A. Traverso, L. Wee, A. Dekker, R. Gillies, Int. J. Radiat. Oncol. Biol. Phys. 102 (2018) 1143–1158.
[180] M. Pozzi, S. Noei, E. Robbi, et al., Sci. Rep. 14 (2024) 28435.
[181] L. Marti-Bonmati, D.M. Koh, K. Riklund, et al., Insights Imaging 13 (2022) 89.
[182] Y. Zhang, G. He, L. Ma, et al., Nat. Commun. 14 (2023) 5798.
[183] C. McCaffrey, C. Jahangir, C. Murphy, et al., Expert Rev. Mol. Diagn. 24 (2024) 363–377.
[184] R. Colling, H. Pitman, K. Oien, et al., J. Pathol. 249 (2019) 143–150.
[185] T. Sakamoto, T. Furukawa, K. Lami, et al., Transl. Lung Cancer Res. 9 (2020) 2255–2276.
[186] A. Shmatko, N. Ghaffari Laleh, M. Gerstung, J.N. Kather, Nat. Cancer 3 (2022) 1026–1038.
[187] Y.P. Zhang, X.Y. Zhang, Y.T. Cheng, et al., Mil. Med. Res. 10 (2023) 22.
[188] C.A. La Porta, S. Zapperi, Cell Rep. Med. 3 (2022) 100851.
[189] L. Wang, K.J. Yoon, IEEE Trans. Pattern Anal. Mach. Intell. 44 (2022) 3048–3068.
[190] M. Ma, Z. Gui, Z. Gao, B. Wang, Sensors 24 (2024) 4127.
[191] J. Hu, Y. Jiang, L. Chen, et al., PLoS One 14 (2019) e0214587.
[192] M. Saha, M. Chakraborty, S. Maiti, D. Das, Neural Comput. Appl. 36 (2024) 20067–20087.
[193] G. Işık, İ. Paçal, Neural Comput. Appl. 36 (2024) 12047–12059.
[194] G.C.M. Siontis, R. Sweda, P.A. Noseworthy, et al., BMJ Health Care Inform. 28 (2021) e100466.
[195] B. Zhou, A. Khosla, A. Lapedriza, et al., Learning deep features for discriminative localization, in: Proceedings of the IEEE Conference on Computer Vision and Pattern Recognition, 2016, pp. 2921–2929.
[196] H.D.A. Dolk, H. Dalianis, T. Vakili, Evaluation of LIME and SHAP in explaining automatic ICD-10 classifications of Swedish gastrointestinal discharge summaries, in: Proceedings of the 18th Scandinavian Conference on Health informatics, 2022, pp. 166–173.
[197] D. Geleta, A. Nikolov, G. Edwards, et al., bioRxiv (2021), doi:10.1101/2021.10.28.466262.
[198] Y. Zhou, X. Shen, Z. He, et al., J. Theory Pract. Eng. Sci. 4 (2024) 45–51.
[199] B.H. Kann, A. Hosny, H.J.W.L. Aerts, Cancer Cell 39 (2021) 916–927.
[200] R. Zhang, Y. Lin, Y. Wu, et al., Brief. Bioinform. 25 (2024) bbae298.
[201] Z. Ding, L. Zhang, Y. Zhang, et al., J. Med. Internet Res. 27 (2025) e55046.
[202] C. Corti, M. Cobanaj, E.C. Dee, et al., Cancer Treat. Rev. 112 (2023) 102498.
[203] H. Alami, P. Lehoux, Y. Auclair, et al., J. Med. Internet Res. 22 (2020) e17707.
[204] G. Chenais, E. Lagarde, C. Gil-Jardiné, J. Med. Internet Res. 25 (2023) e40031.
[205] W.Z. Bu Qingfeng, Li Qi, He Chuting, et al., Soc. Med. Health Manag. 4 (2023), doi:10.23977/socmhm.2023.040209.
[206] A. Brauneck, L. Schmalhorst, M.M. Kazemi Majdabadi, et al., J. Med. Internet Res. 25 (2023) e41588.
[207] D. Froelicher, J.R. Troncoso-Pastoriza, J.L. Raisaro, et al., Nat. Commun. 12 (2021) 5910.
[208] L. Carvalho Martins, E.A. Cino, R.S. Ferreira, J. Chem. Theory Comput. 17 (2021) 4262–4273.
[209] M.S. Hussain, P.S. Ramalingam, G. Chellasamy, et al., Clin. Breast Cancer 25 (2025) 406–421.
[210] Q. Zeng, C. Chen, C. Chen, et al., Spectrochim. Acta Part A 286 (2023) 122000.
[211] X. Ma, H. Cheng, J.W. Hou, et al., Chin. Opt. Lett. 18 (2020) 051701.
[212] H. Yuan, Y. Chen, Y. Hu, et al., J. Pharm. Investig. 55 (2025) 889–902.
[213] G. Khan, M.S. Hussain, S. Ahmad, et al., Naunyn-Schmiedeberg's Arch. Pharmacol. 398 (2025) 13351–13370.
[214] J. Pang, N. Ding, X. Liu, et al., Ann. Surg. Oncol. 32 (2025) 750–759.